

Utilizing Advanced Cell Models to Investigate Neurological Diseases and Find Potential Therapies

Expert Insights

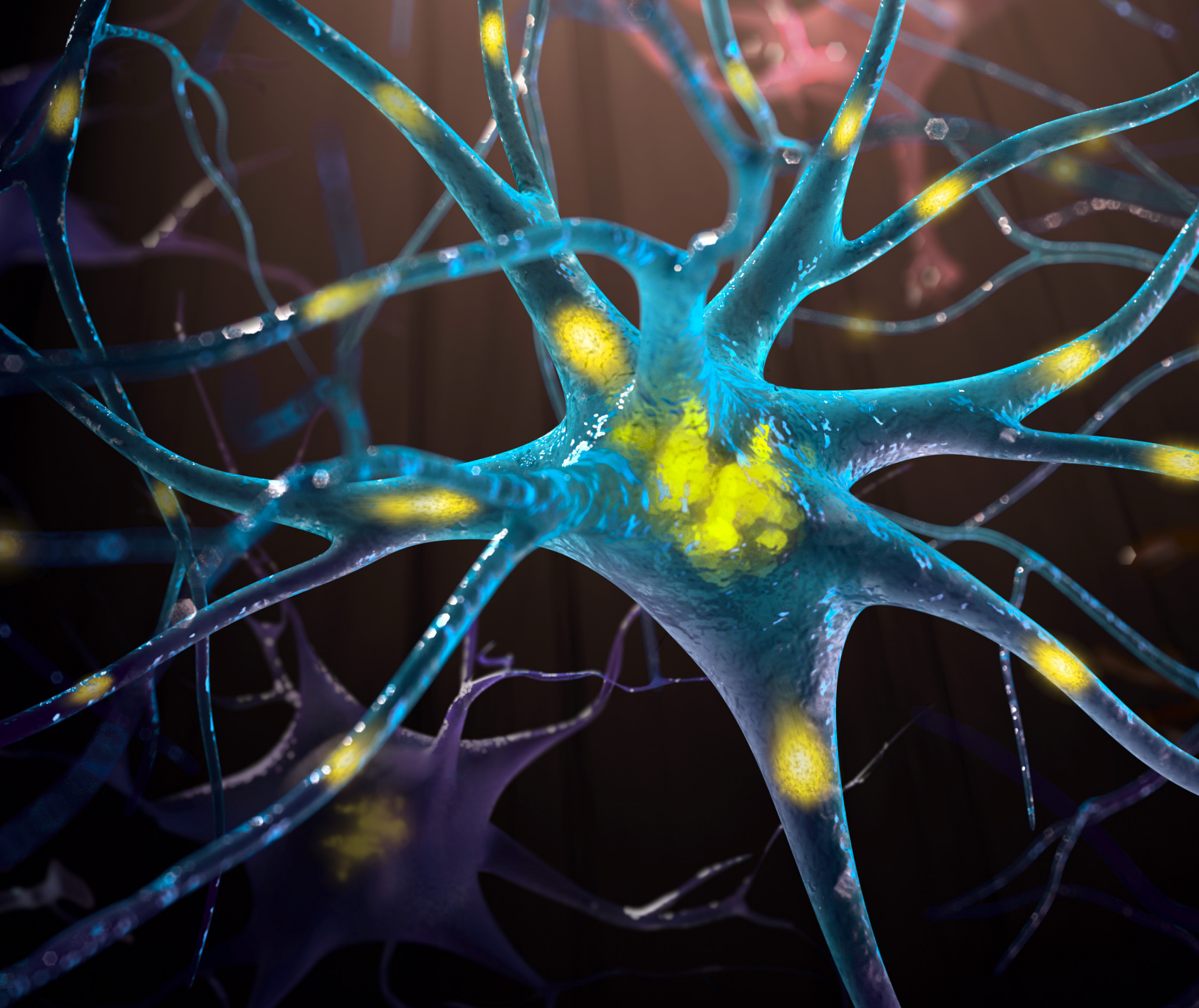


Sponsored by:

SARTORIUS

**CURRENT
PROTOCOLS**
A Wiley Brand

WILEY



Fast Track Scientific Discovery With Incucyte® Live-Cell Analysis

The Incucyte® Live-Cell Analysis System speeds scientific discovery by combining lab-tested protocols and reagents with powerful, automated image acquisition and analysis. Gain dynamic insights into the health, morphology, movement and function of cell models, all from the stable environment of a tissue culture incubator.



Select an Incucyte® for Your Research

Simplifying Progress

SARTORIUS

Contents

4 Introduction

7 Neuroprotective potential of choline alfoscerate against β -amyloid injury: Involvement of neurotrophic signals
Adapted from Catanesi et al.

10 Studying human neurological disorders using induced pluripotent stem cells: From 2D monolayer to 3D organoid and blood-brain barrier models
Adapted from Logan et al.

14 Improving *in vitro* models for Alzheimer's disease
Whitepaper by Alcantara et al.

23 Optimization of SH-SY5Y differentiation using growth factors and cytokines
Application note by Trigg et al.

34 Quantifying chemotherapeutic cytotoxicity in glial cells using AI-driven label-free cell analysis
Application note by Trigg et al.

44 iPSC-derived motor neurons and microglia from ALS background display disease phenotype
Whitepaper by Jessica Tilman

Imprint

©John Wiley & Sons, Inc.
111 River Street,
Hoboken, NJ 07030-5774
USA
Contact: [Customer Service](#)

Editors:
Róisín Murtagh
Dr. Birgit Folta

Senior Account Manager:
Joseph Tomaszewski

Sartorius
<https://www.sartorius.com/>

Introduction

Neurological diseases, including neurodegenerative and developmental diseases, as well as neuro-oncology, are complex and require a multidisciplinary approach to diagnosis and management. Research efforts aimed at understanding the underlying causes of these diseases and developing novel treatment strategies are ongoing. Early diagnosis, better understanding of disease mechanisms, and advancements in therapeutic interventions hold promise for improving patient outcomes and quality of life in the future.

Neurodegenerative diseases are characterized by the progressive degeneration and death of nerve cells in the brain and/or spinal cord. These diseases often result in the gradual decline of cognitive and motor functions over time. Examples of neurodegenerative diseases include Alzheimer's disease (AD), Parkinson's disease, Huntington's disease, and amyotrophic lateral sclerosis (ALS). These conditions, for which there is currently no cure, are typically caused by a combination of genetic and environmental factors. Treatments for these diseases typically focus on managing symptoms and improving the quality of life for patients.

Developmental diseases, on the other hand, are conditions that arise during early development and can affect the structure and function of the nervous system. Autism spectrum disorders and cerebral palsy, for example, can be genetic or caused by external factors, such as infection or exposure to toxins during gestation. The specific symptoms and severity of these diseases can vary widely depending on the underlying cause and affected areas of the brain.

Neuro-oncology is a subspecialty of neurology that focuses on the diagnosis and treatment of brain and spinal cord tumors. These tumors can be either benign or malignant, and they can originate in the brain or spread from other parts of the body. The field of neuro-oncology is rapidly evolving, with advancements in imaging technologies and targeted therapies offering new hope for patients.

In vitro cellular models in 2D, as well as 3D in the form of brain organoids, are available for investigating neurological diseases. Constant observation and analysis under as many physiological conditions as possible are particularly important for this since human cells, such as primary or induced pluripotent stem cells (iPSCs), react very sensitively to changes in culture conditions. Technological progress has greatly simplified the robust culture and analysis of these precious advanced cell models. In particular, the development of label-free analytical techniques, which negate the requirement of fluorescence labels, enables research of physiologically relevant processes in disease development and progression without any artifacts being introduced by the fluorescent label or labeling process.

This Expert Insight begins with a summarized study on the role of α -GPC in AD from Catanesi *et al.* [1]. AD is characterized by chronic progression of cognitive and memory impairment, which is associated with lower choline and phospholipids in postmortem AD brains. The phosphatidylcholine derivative, choline alfoscerate (L-alpha-glycerylphosphorylcholine [α -GPC]) upregulates acetylcholine in the hippocampus. The authors utilize *in vitro* human AD models with live-cell analysis to investigate the molecular mechanisms underlying the α -GPC-induced reduction of cognitive decline.

In the second summarized article, Logan *et al.* [2] present the use of iPSCs to generate 2D, 3D, and blood-brain barrier (BBB) models to investigate mechanisms of neurological disorders and for screening therapeutic candidates. Current animal models do not appear to sufficiently mimic human diseases. iPSCs can be derived from patients with neurological disease and therefore they represent a human *in vitro* model. For using iPSC-based cell models it is important to monitor cell viability, morphology, changes in protein expression, and action potentials over days.

The whitepaper from Alcantara *et al.* describes the improvement of an *in vitro* cell model to study AD. The authors analyzed 2D and 3D cell models of patient-derived iPSC cell and used live-cell imaging under controlled environmental conditions which give critical dynamic insight into cell morphology, function, and cell/cell interactions, and enables the study of chronic diseases where cells change slowly, such as AD.

SH-SY5Y cells, which exist as two morphologically distinct phenotypes including epithelial-like (S-type) or neuroblast-like (N-type), are a subclone of the human SK-N-H parental neuroblastoma cell line. They are a widely used *in vitro* model as they can be differentiated into a neuronal-like phenotype. In an application note by Trigg *et al.*, a robust differentiation of human SH-SY5Y cells into neuronal-like cells using specific growth factors and cytokines is presented. Live-cell imaging is used to visualize and quantify changes in proliferation, morphology, and cell surface antigen expression.

In an application note by Trigg *et al.*, a neuroblastoma cell model has been used to analyze cell death in response to cytotoxic compounds and drug sensitivity to different chemotherapeutics. Neuro-oncology research often relies on tumor cell lines such as neuroblastomas or glioblastomas, but these cell lines do not represent the complexity and heterogeneity observed in brain tumors, therefore the authors performed cell health analysis with live-cell imaging using drug-treated primary rat astrocytes. They also demonstrate a combined approach to quantify cell death in microglia using live-cell analysis and flow cytometry.

Finally, in an application note by Tilman, a cell model of ALS has been investigated. Fibroblasts taken from a healthy individual and an ALS patient carrying a C9orf72 hexanucleotide expansion were reprogrammed to iPSCs and differentiated to motor neurons and microglia alongside controls. The cells were then assessed for differences in morphology and functional activity measured via different assays using live-cell analysis methods.

In summary, these articles show that the non-perturbing analysis of advanced cell models, such as primary or iPSC-derived cell types, is important for the research on neurological diseases to better understand their development, progression, and treatment. In this context, live-cell imaging is a helpful tool to temporally investigate cellular changes in 2D or 3D robustly without further influences.

Through the methods and applications presented in this Expert Insights, we hope to educate researchers on new technologies and techniques for analyzing *in vitro* cell models. For more information, we encourage you to visit [Sartorius](#) to learn more and explore options to enhance your research.

Dr. Birgit Foltas

Editor at Wiley Analytical Science

References

- [1] Catanesi, M. et al. (2020). Neuroprotective potential of choline alfoscerate against β -amyloid injury: Involvement of neurotrophic signals. *Cell Biology International*. DOI: 10.1002/cbin.11369.
- [2] Logan, S. et al. (2019). Studying Human Neurological Disorders Using Induced Pluripotent Stem Cells: From 2D Monolayer to 3D Organoid and Blood Brain Barrier Models, in *Comprehensive Physiology*. DOI: 10.1002/cphy.c180025

Neuroprotective potential of choline alfoscerate against β -amyloid injury: Involvement of neurotrophic signals

Adapted from Catanesi et al., 2020

The global prevalence of Alzheimer's disease (AD) and inadequate responses to current therapies warrant new approaches to drug discovery. AD is characterized by chronic progression of cognitive and memory impairment, which is associated with lower choline and phospholipids in postmortem AD brains. The phosphatidylcholine derivative, choline alfoscerate (L-alpha-glycerylphosphorylcholine [α -GPC]) up-regulates acetylcholine in the hippocampus. Treatment with α -GPC has improved memory in clinical trials of stroke patients and early AD patients. This research investigates the molecular mechanisms of α -GPC that may reduce cognitive decline in *in vitro* human models of AD.

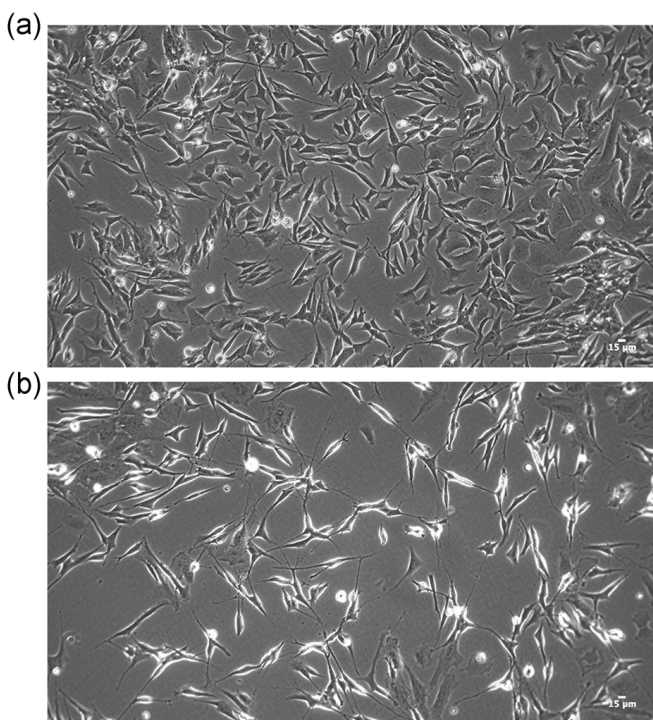


Figure 1. Phase-contrast microscopy of SH-SY5Y cells. (a) SH-SY5Y incubated in control media for 72 hours (non-differentiated cells) (b) SH-SY5Y treated with all-trans retinoic acid (ATRA) for 72 hours (differentiated cells). ATRA treatment yielded consistent differentiation of SH-SY5Y cells into neuronal-like cells.

Introduction

AD is associated with cholinergic dysfunction, reduced phospholipid and methyl-group metabolism, and decreased synaptic formation and function. AD often shows a reduction in cholinergic neurons in the basal forebrain. Cholinergic neurons in the basal forebrain require nerve growth factor (NGF) to survive during development and maintain the cholinergic phenotype during adulthood. Amyloid pathologies and AD are associated with impaired pathways of NGF maturation and brain-derived neurotrophic factor (BDNF). NGF and BDNF play critical roles in multiple cellular processes including differentiation, maintenance of synaptic connections, activity-dependent plasticity, and suppression of apoptosis. Although α -GPC has been shown to ameliorate cognitive decline in multiple patients with stroke or AD in clinical trials, its mechanisms for improving cognitive function remain elusive. This research utilizes *in vitro* human AD models with microscopy and end-point biochemical assays to investigate the molecular mechanisms underlying the α -GPC-induced reduction of cognitive decline.

Differentiation into neuronal-like cells

Human neuroblastoma SH-SY5Y cells were incubated with all-trans retinoic acid (ATRA) in cell culture media for 72 hours. The SH-SY5Y cells were differentiated into a neuronal-like phenotype with ATRA in a reproducible manner, as shown in representative images (Fig. 1).

Effect of α -GPC on beta-amyloid-induced injury in early and preventive Alzheimer's disease models

After ATRA treatment for 72 hours, two models were used to assess the effects of α -GPC on the injury of these differentiated SH-SY5Y cells to oligomeric β -amyloid (1-42). In the early model (model 1), differentiated cells were incubated with fresh media containing oligomeric β -amyloid (1-42) for 1 hour followed by the addition of various concentrations of α -GPC for 24 hours. This early *in vitro* model attempts to mimic the early stages of AD when patients have mild cognitive impairment. It provides a platform for investigating the effects of α -GPC on the progression of the disease.

The second *in vitro* model investigates the potential preventive effects of α -GPC against neurodegeneration. After differentiation, the cells were incubated in fresh media containing various concentrations of α -GPC for 24 hours. Subsequently, oligomeric β -amyloid (1-42) was added to cells and incubated for 24 hours. The effect of α -GPC on the β -amyloid exposure in models 1 and 2 are shown in Figure 2. The control cells (Ctr) were incubated in fresh media and were not exposed to oligomeric β -amyloid (1-42) nor α -GPC.

Cell viability in both models was significantly reduced by treatment with β -amyloid (1-42) (Fig. 2). Treatment with solely α -GPC at any concentration did not affect the viability of the cells (Fig. 2). After the 1 hour exposure to β -amyloid (1-42), α -GPC treatment for 24 hours improved the viability of the β -amyloid-injured cells (Fig. 2a). Pretreatment of the neuronal-like cells with α -GPC at any concentration before β -amyloid injury significantly increased the viability of the cells. These results suggest that α -GPC can significantly prevent the death of some cells from β -amyloid-induced injury (Fig.

2b). The lack of a dose-response curve for α -GPC indicated that the lowest tested dose of α -GPC was sufficient to ameliorate or prevent many of the effects of β -amyloid injury on these neuronal-like cells. Thus, the lowest dose of α -GPC was used in subsequent experiments. However, the mechanism of β -amyloid-induced death was not revealed by this assay.

Several types of cell death are feasible: apoptosis, necrosis, and ferroptosis. Differentiated cells treated in the two *in vitro* AD models were assessed for the apoptosis-associated proteins, procaspase-9, cleaved caspase-9, and JNK by western blot technique. The results indicated that α -GPC treatment in the preventive models significantly reduced the production of cleaved caspase-9 and JNK, strongly suggesting a major role of apoptosis in the β -amyloid-induced injury of the neuronal-like cells. The results in the preventive model also suggested that α -GPC thwarted the β -amyloid-induced injury in many neuronal-like cells.

To corroborate the role of apoptosis in β -amyloid-induced injury, the early *in vitro* AD model and the preventive AD model were assessed for Annexin V response using the Incucyte¹ Live-Cell Analysis System (Sartorius). Live-cell analysis of the early *in vitro* AD model showed that β -amyloid treatment increased Annexin V positive staining (green fluorescence) and that α -GPC treatment significantly reduced the number of Annexin V positive cells (Fig. 3a). Furthermore, the preventive *in vitro* AD model showed that α -GPC pretreatment significantly reduced the number of β -amyloid injured cells staining positive for Annexin V, suggesting that α -GPC pretreatment can

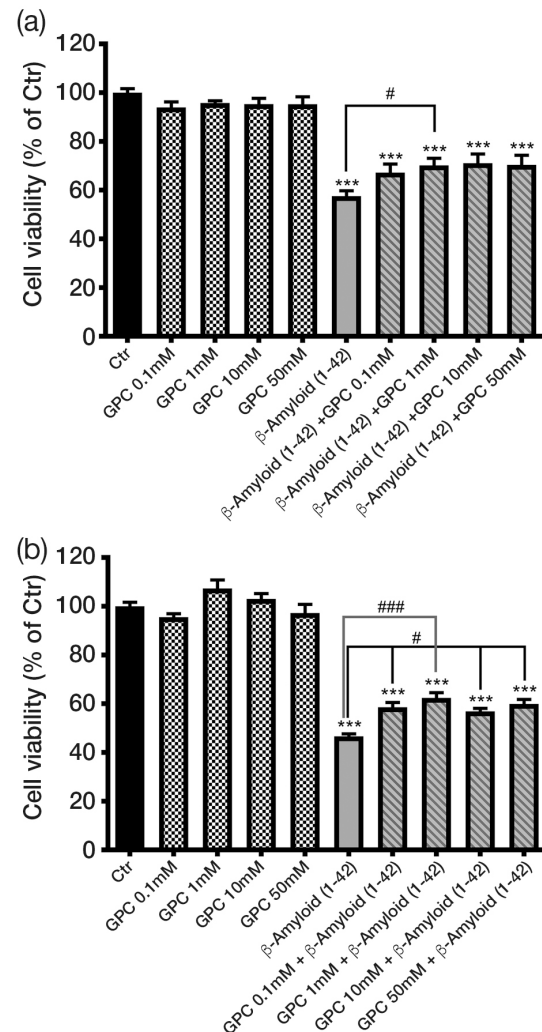
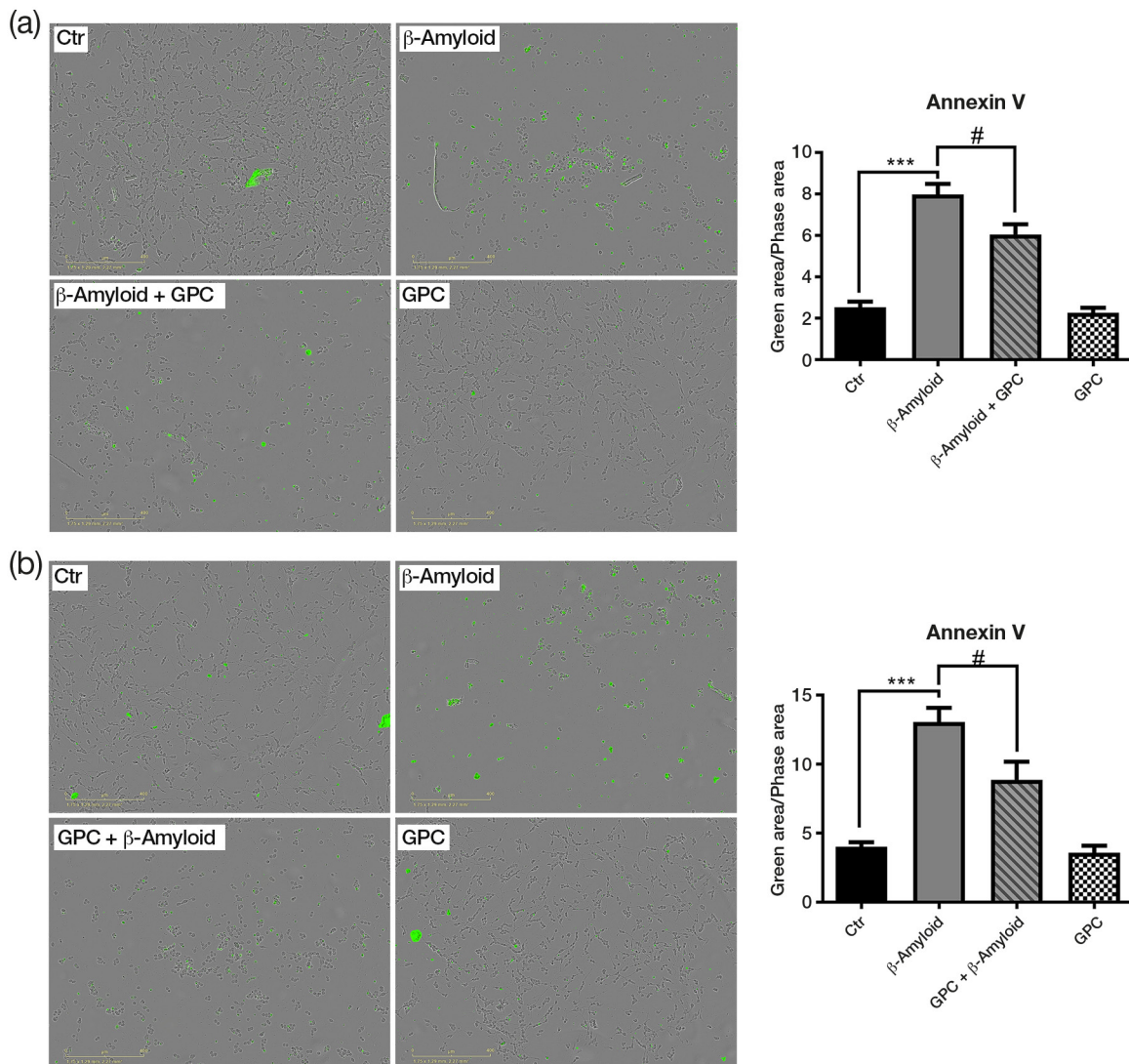


Figure 2. Viability of differentiated SH-SY5Y cells receiving no treatment (Ctr), indicated concentrations of α -GPC, and/or oligomer β -amyloid (1-42). (a) Effect of indicated α -GPC concentrations administered after β -amyloid (1-42) injury. (b) Effect of indicated α -GPC concentrations administered 24 hrs before β -amyloid (1-42) injury. Data reported as mean \pm SEM of three distinct experiments. Significance was calculated with one-way analysis of variance (ANOVA) with Tukey's post hoc test. Control (Ctr) vs treatments ** p <0.001, * p <0.0001; β -amyloid (1-42) vs β -amyloid (1-42) + α -GPC: # p <0.05. α -GPC, L-alphaglycerylphosphorylcholine; Ctr, control; SEM, standard error of mean.**

prevent β -amyloid injury (Fig. 3b).

The effects of α -GPC on neurite length were explored in both amyloid β -induced injury models. Amyloid β -treated neuronal-like cells significantly decreased neurite length in both models. Treatment with α -GPC either before or 1 hour after amyloid β injury significantly hindered the amyloid β -induced reduction of neurite length, further supporting the protective and rescuing role of α -GPC.



*Figure 3. Annexin V Green staining evaluated by an Incucyte Live-Cell Analysis System in both in vitro β-amyloid injury models. (a) Effect of α-GPC administered after β-amyloid (1-42) injury. (b) Effect of α-GPC administered 24 hrs before β-amyloid (1-42) injury. Data reported as mean ± SEM of three distinct experiments. Significance was calculated with one-way ANOVA and Tukey's post hoc test. Control (Ctr) vs treatments ***p<0.0001; β-amyloid (1-42) vs β-amyloid (1-42) + α-GPC: #p<0.05. α-GPC, L-alpha-glycerylphosphorylcholine; Ctr, control; SEM, standard error of mean.*

In addition, amyloid β is known to downregulate the prosurvival pathway (p-AKT/p-TRKB/mBDNF/ERK5) in neuronal cells. Treatment with α-GPC before or after 1 hr amyloid β injury significantly protected or rescued the prosurvival pathway, respectively, as determined by western blot analysis.

In summary, α-GPC treatment before or 1-hour post amyloid β-induced injury provided protective and rescue effects in neuronal-like cells, respectively, as demonstrated by morphology, cell viability, reduced

apoptosis, and rescued neurite length, and prosurvival pathways by multiple methods. The live-cell analysis techniques demonstrate how researchers can monitor the percentage of cell differentiation, cell health, and morphology coupled with prespecified pretreatment over time to investigate neurotoxin-induced injury and screen and/or characterize the effects of one or more neuroceuticals, medications, and potential drug candidates for neurological disorders.

Studying Human Neurological Disorders Using Induced Pluripotent Stem Cells: From 2D Monolayer to 3D Organoid and Blood-Brain Barrier Models

Adapted from Logan et al., 2019

Neurological disorders can severely affect the quality of life. Their global prevalence is a major healthcare concern: Development of new therapeutics is vital but current animal models do not sufficiently mimic human diseases. Induced pluripotent stem cells (iPSCs) grown from the tissue of healthy humans and humans with neurological disorders are invaluable tools for modeling neurological disorders. iPSCs can self-renew and have unlimited capacity to differentiate into multiple types of neural cells such as neurons, glial cells, oligodendrocytes, and brain microvascular epithelial cells (BMECs). This review describes the use of iPSCs to generate two-dimensional (2D), three-dimensional (3D), and blood-brain barrier (BBB) models for revealing cellular, molecular, and genetic mechanisms of neurological disorders and screening therapeutic candidates.

Introduction

Many neurological disorders, such as neurodegenerative, neurodevelopmental, and psychiatric disorders, are increasingly becoming major healthcare concerns due to their impact on quality of life and worldwide prevalence. The causes of neurological disorders involve complex interactions between environmental factors and genetics: they are not well understood. Animal models have played a major role in studying neurological disorders, however inherent limitations of these models such as species differences, imperfect replication of human disease phenotypes, and ethical concerns have contributed to high failure rates in translating promising animal research findings to successful therapeutic

interventions in humans. The continuing development of translational human models of neurological disorders using iPSCs expands research for identifying mechanisms of disease onset and progression and for assessing therapeutic candidates in conditions that recapitulate human disease.

Most iPSCs are derived from skin fibroblasts, blood cells, or urine cells grown with specific growth factors and conditions in a process called reprogramming (Fig. 1). Because iPSCs can be derived from patients who have a neurological disorder, scientists can use these iPSCs and their differentiated cells to study the role of genetic factors, environmental issues, and longitudinal changes in an endogenous human *in vitro* model of the disease.

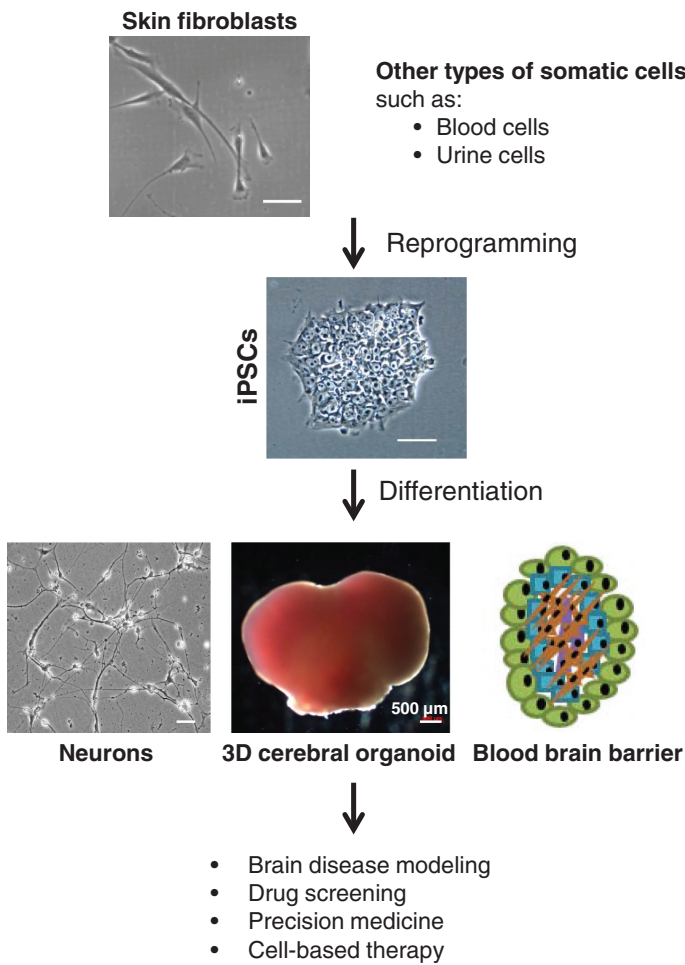


Figure 1. Generation and applications of induced pluripotent stem cells (iPSCs). Human iPSCs can be derived from multiple somatic cells and subsequently differentiated into neuronal cell types in a monolayer culture (2D) and in organoids (3D). iPSCs also can be differentiated into four cell types and cultured together to provide a blood-brain barrier (BBB) model. Scale bars with no labels: 20 μ m.

Generation of different brain cells from iPSCs in 2D Monolayer cultures

Neural cells

Neural stem cells (NSCs) can be differentiated into seven types of neurons: motor neurons, dopaminergic neurons, GABAergic neurons, pyramidal neurons, serotonergic neurons, and nociceptor neurons. Dysfunction of each type of neuron is associated with specific diseases (Fig. 2).

Non-neuronal iPSC-induced neural cells

iPSCs also can differentiate into the additional six types of brain cells: neural stem cells [1], astrocytes [2], oligodendrocytes, microglia [3–5], BMECs, and pericytes (Fig. 2).

Published protocols for differentiating iPSCs to specific neurons or non-neuronal cells in-

volve growth factors and activation and/or inhibition of specific proteins for each cell type.

The reproducibility of iPSC differentiation into the various brain cells depends on phenotypic assessments while minimizing artifacts introduced by the manipulation of culture vessels. Many laboratories are using live-cell analyses utilizing purpose-built systems such as the Incucyte Live-Cell Analysis System [1,4–9] that can assess cellular morphology by phase contrast and various fluorescent markers at specified time intervals while the culture plates remain in the specialized incubator for days to months which minimizes artifacts, reduces resources, and improves reproducibility. Subsequent bioassays can investigate the morphology and physiology under relevant conditions [6]

(e.g., titration of stimulants or specific neurotoxins) and further expand the neuroscientists' research tools [5]. iPSCs derived from patients with brain diseases or specific variants are used to develop *in vitro* 2D assays for investigating various brain diseases [10].

3D cultures or organoids from iPSCs

Organoids are 3D structures containing several types of cells that self-organize and can perform at least one function of the organ. Human cerebral organoids contain iPSC-differentiated neurons, oligodendrocytes, and astrocytes. The neurons can provide spontaneous calcium surges and action potentials, demonstrating their functional activity [6]. Live-cell analyses using the Incucyte Live-Cell Analysis System and integrated software enables the visualization and quantification of several 3D cultures including organoids, for example assessing including cell growth, phenotype, and morphological changes [10–13].

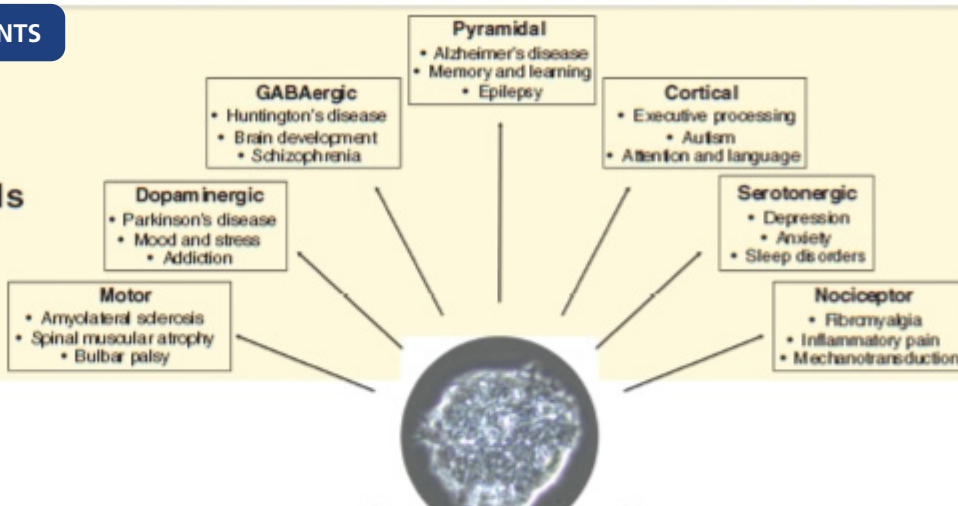
Blood-brain barrier models

Human iPSCs can be differentiated into four cell types (astrocytes, neurons, pericytes, and brain microvascular endothelial cells (BMECs)) to generate BBB models, which exist in 2D or 3D. BBB models support the study of environmental factors on neurodegenerative diseases such as extracellular vesicles containing β -amyloid from brain cerebral microvascular endothelial cells [1]. These results support using a BBB model for further mechanistic studies and potentially as a screen for potential therapeutic agents. Live-Cell Analysis can be utilized in monitoring changes during 2D cell culture or differentiation, such as cell viability, morphology, or changes in cell surface protein expression [1].

Modeling neurodegenerative diseases

Human iPSC-based models of neurodegenerative diseases include Alzheimer's disease (AD) [1,5,8,14], amyotrophic lateral sclerosis with frontotemporal dementia (ALS/FTD) [15], Parkinson's disease (PD) [13], Huntington's disease (HD), and Gaucher's disease (GD) [10]. Human iPSC-derived models also investigate neurodevelopmental disorders (e.g., autism spectrum disorder [11,12]) and psychiatric disorders (e.g., schizophrenia [12], bipolar disorder).

Neuronal cells



iPSCs

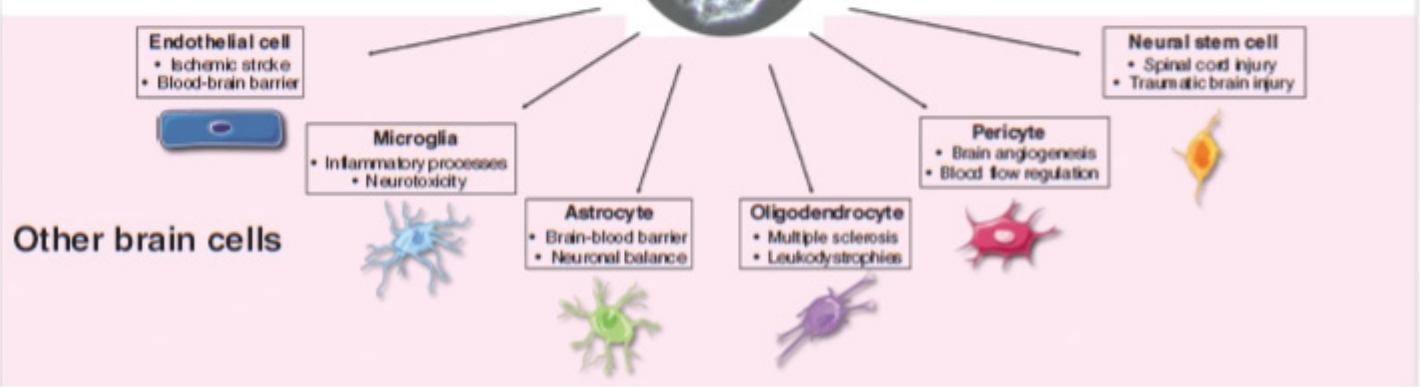


Figure 2. iPSCs can differentiate into numerous types of brain cells. Their key role in brain physiology and their association with brain disorders are included. Top panel: Seven types of neurons differentiated from iPSCs. Bottom panel: Six types of non-neuronal brain cells differentiated from iPSCs.

Drug screening and discovery

Screening for drug toxicity (e.g., anesthetic exposure, addiction) has mostly used the 2D models. Screening for drug efficacy and precision medicine often utilizes iPSCs derived from the patient and the relevant model (2D, 3D, BBB) [14,15].

Advantages and limitations of 2D monolayer, 3D organoid, and BBB cultures

Human iPSC-derived 2D, 3D organoid, and BBB models enable longitudinal studies on the maturation of neural cells and progression of disease, mechanistic studies linking pathology with molecular profiles, and cellular interaction studies elucidating the contributions of individual risk factors and specific cell types to disease. Live-cell analysis reduces resources, minimizes artifacts, and improves reproducibility and productivity while assessing cellular health, morphology, protein expression, and physiology under relevant conditions in human *in vitro* models of neurological disorders [1,4–9].

The 2D model is the most widely used iP-

SC-based approach for investigating cell-specific morphology and physiology in brain diseases due to cost and high throughput potential for drug screening [3]. Different types of neural cells grown in 2D monolayer cultures can be combined to generate organoids and BBB models. Limitations of the 2D monoculture system include the time-consuming process from primary cells to iPSCs to differentiated cells and the neural cells resemble fetal brain cells.

Organoids or 3D models contain several relevant types of brain cells, so it supports cellular interaction studies. Organoids do not yet include vascularization, so its center eventually becomes necrotic due to lack of nutrients.

In comparison to 2D monolayers and 3D organoids, researchers can investigate the contributions of environmental factors to phenotype, manipulate those environmental factors, observe the flux of substrates, and probe the role of specific transporters in BBB models. Limitations of BBB models include higher costs and technical challeng-

es. Opportunities for improving BBB models include the addition of vascularization which may enable fluctuation of perfusion rate and shear stress, thereby more closely mimicking the BBB *in vivo*.

In summary, iPSCs derived from cells from patients with multiple neurological disorders enable the development of *in vitro* translational human models for elucidating mechanisms of disease onset and progression as well as screens for potential new treatments. Disease models range from 2D monolayer cultures to 3D organoid models to BBB models. Many researchers are using live-cell analyses such as the Incucyte Live-Cell Analysis System [1,4–9] to monitor cellular morphology by phase contrast, expression of specific proteins via various fluorescent markers, and stimulant or neurotoxin-induced changes in physiology at their designated time intervals while minimizing artifacts, reducing resources, and improving reproducibility. Herein, a combination of models is recommended to elucidate the underlying mechanisms of human brain diseases and pathological phenotypes.

References

- [1] Osborne, O.M. et al. (2022). Brain endothelium-derived extracellular vesicles containing amyloid-beta induce mitochondrial alterations in neural progenitor cells. *Extracellular Vesicles and Circulating Nucleic Acids*. DOI: 10.20517/evcna.2022.22.
- [2] Barbar, L. et al. (2020). CD49f Is a Novel Marker of Functional and Reactive Human iPSC-Derived Astrocytes. *Neuron*. DOI: 10.1016/j.neuron.2020.05.014.
- [3] Breitmeyer, R. et al. (2023). Regulation of synaptic connectivity in schizophrenia spectrum by mutual neuron-microglia interaction. *Communications Biology*. DOI: 10.1038/s42003-023-04852-9.
- [4] McQuade, A. et al. (2020). Gene expression and functional deficits underlie TREM2-knockout microglia responses in human models of Alzheimer's disease. *Nature Communications*. DOI: 10.1038/s41467-020-19227-5.
- [5] Reich, M. et al. (2021). Alzheimer's Risk Gene TREM2 Determines Functional Properties of New Type of Human iPSC-Derived Microglia. *Frontiers in Immunology*. DOI: 10.3389/fimmu.2020.617860.
- [6] Wang, J. et al. (2023). Organelle mapping in dendrites of human iPSC-derived neurons reveals dynamic functional dendritic Golgi structures. *Cell Reports*. DOI: 10.1016/j.celrep.2023.112709.
- [7] Fumagalli, L. et al. (2021). C9orf72-derived arginine-containing dipeptide repeats associate with axonal transport machinery and impede microtubule-based motility. *Science Advances*. DOI: 10.1126/SCIADV.ABG3013.
- [8] Lagomarsino, V.N. et al. (2021). Stem cell-derived neurons reflect features of protein networks, neuropathology, and cognitive outcome of their aged human donors. *Neuron*. DOI: 10.1016/j.neuron.2021.08.003.
- [9] Ihry, R.J. et al. (2018). P53 inhibits CRISPR-Cas9 engineering in human pluripotent stem cells. *Nature Medicine*. DOI: 10.1038/s41591-018-0050-6.
- [10] Baden, P. et al. (2023). Glucocerebrosidase is imported into mitochondria and preserves complex I integrity and energy metabolism. *Nature Communications*. DOI: 10.1038/s41467-023-37454-4.
- [11] Frei, J.A. et al. (2021). Regulation of neural circuit development by cadherin-11 provides implications for autism. *eNeuro*. DOI: 10.1523/ENEURO.0066-21.2021.
- [12] Tai, D.J.C. et al. (2022). Tissue- and cell-type-specific molecular and functional signatures of 16p11.2 reciprocal genomic disorder across mouse brain and human neuronal models. *American Journal of Human Genetics*. DOI: 10.1016/j.ajhg.2022.08.012.
- [13] Ryan, S.K. et al. (2023). Microglia ferroptosis is regulated by SEC24B and contributes to neurodegeneration. *Nature Neuroscience*. DOI: 10.1038/s41593-022-01221-3.
- [14] Bassil, R. et al. (2021). Improved modeling of human AD with an automated culturing platform for iPSC neurons, astrocytes and microglia. *Nature Communications*. DOI: 10.1038/s41467-021-25344-6.
- [15] Szebényi, K. et al. (2021). Human ALS/FTD brain organoid slice cultures display distinct early astrocyte and targetable neuronal pathology. *Nature Neuroscience*. DOI: 10.1038/s41593-021-00923-4.

Keywords or phrases:

Cell Analysis, Alzheimer's, *in vitro*, Progressive Disease, Reagents, Tau Peptide, Neuro-inflammation

Improving *in vitro* models for Alzheimer's disease

Susana L Alcantara², Belinda Oclair¹, Kalpana Barnes², Timothy Dale²

¹ Sartorius Corp. 300 West Morgan Road, Ann Arbor, Michigan, 48108, USA

² Sartorius UK Ltd., Units 2 & 3 The Quadrant, Newark Close, Royston Hertfordshire SG8 5HL UK

Correspondence

E-Mail: askascientist@sartorius.com

Introduction

Alzheimer's disease (AD) is a progressive, chronic neurodegenerative disease. It generally begins with poor recollection of recent events, then progresses to more severe memory loss, personality and behavioral changes (such as paranoia and agitation), and difficulty in performing everyday tasks. At its most severe, AD patients require around-the-clock care, as they are incapable of carrying out the basic activities of daily living. In an aging global population, the incidence of AD is steadily rising. It is estimated that 50 million people were living with dementia in 2017 – equating to an estimated 5.6 million people over age 65 living with AD in the USA alone – and the annual number of new cases of AD and other dementias is projected to double by 2050.^{1,2}

AD can be devastating to both patients and their families, with the necessary long-term care estimated to have cost \$290 billion in the USA in 2019.³ And this figure does not include the unpaid care often provided by family and friends – the value of which could be up to an additional \$234 billion. This makes the overall financial burden of AD incredibly significant on both a personal and national level, and those costs are only likely to rise. As a result, there is growing investment and research interest in AD, with many academic and industry research groups around the world working to identify effective treatments for the disorder.

Understanding AD

Alois Alzheimer first described the histopathology of AD in 1907.⁴ The disease is characterized by brain atrophy, amyloid plaques (extracellular deposits of amyloid-β (Aβ) peptide aggregates), neurofibrillary tangles (NFTs) (composed largely of tau protein), loss of neurons and synapses, and dystrophic neurites.⁵ The problem is that, while these alterations in synaptic structure and function can be observed in postmortem tissue of patients with AD, it is difficult to determine the complex underlying mechanisms that lead to disease onset and progression. This is further complicated by the fact that processes such as tau hyperphosphorylation and aggregation can produce a range of different effects at various stages of the disease.

Hyperphosphorylation in tau-mediated neurodegeneration

Many neurodegenerative disorders are characterized by the abnormal formation and aggregation of filamentous proteins in the brain.^{5,6} Tauopathies, such as AD, Parkinson's disease (PD), or frontotemporal dementia (FTD) are associated with the hyperphosphorylation and consequent misfolding of the protein tau. In healthy individuals, tau is responsible for the polymerization and stabilization of microtubules, and regulation of axonal transport. In AD and other tauopathies, tau becomes hyperphosphorylated, and is no longer able to bind to microtubules. Instead, it becomes sequestered into NFTs and accumulates in neurons, as well

as in glial tangles in astrocytes or oligodendroglia. Loss of normal tau microtubule-stabilizing function leads to pathological disturbance of the normal structure and regulatory function of the cytoskeleton, affecting both axonal transport and synaptic function and, ultimately, contributing to neurodegeneration. This makes tau hyperphosphorylation a key target for therapeutic intervention.

Several pathogenic events have been linked, either directly or indirectly, to tau hyperphosphorylation, misfolding and aggregation. Recent studies have suggested that axonal transport defects, synapse loss and neuroinflammation may be among the earliest signs of neurodegeneration resulting from tau hyperphosphorylation, whereas fibrillar tau tangles may be late-stage manifestations that physically interfere with normal cellular functions.⁵ Despite the clear involvement of these pathological processes in tau-mediated neurodegeneration, their positioning in the cascade of events that leads to neuronal loss remains unclear, and further investigation is required to fully understand this mechanism. Elucidating the exact roles of the different aggregates and their precursors in neurodegeneration is a challenging endeavor, but one that is likely to remain the focus of future research efforts to discover the mechanisms of disease pathology, as well as to develop better diagnostic and therapeutic tools.

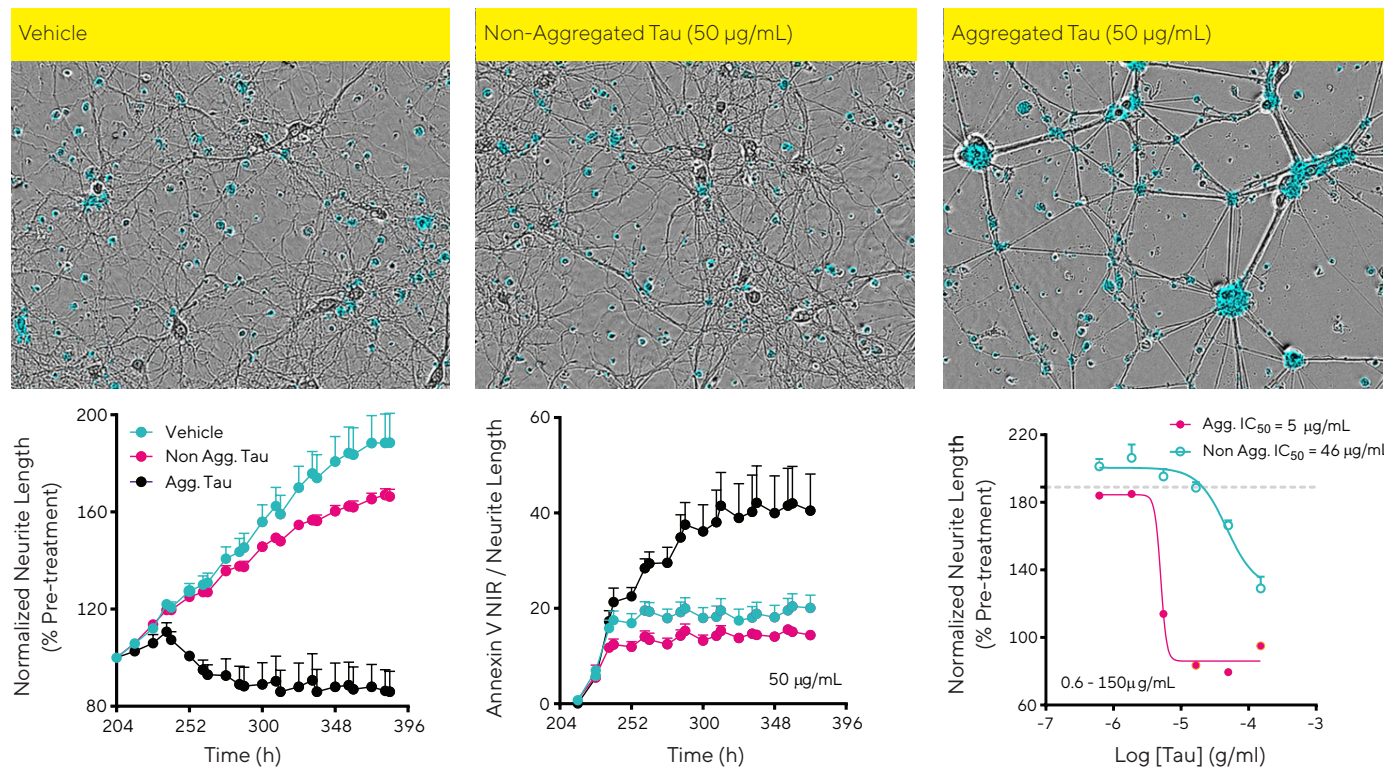


Figure 1: Chronic *in vitro* model of aggregated tau peptide-induced neurotoxicity: Incucyte® primary rat cortical neurons (rCortical) were seeded in PDL-coated 96-well plates at 20,000 cells/well and placed in an Incucyte® Live-Cell Analysis System for the duration of the study. Eight days post-seeding, cells were treated with solubilized or aggregated tau (heparin 4:1 ratio, 37 °C with sporadic rotation for five days) in media containing the apoptotic marker annexin V-NIR (0.25 µg/ml). Kinetic quantification of neurite outgrowth and cell health was performed. Time-courses and concentration curves showed that aggregated tau yielded a concentration-dependent decrease of neurite length (80 ± 5 % vs. 166 ± 3 %, 2-3 replicates) and an increase in cell death (40 ± 8 % vs. 14 ± 1 %, 3 replicates), compared to vehicle. Non-aggregated tau only yielded substantial inhibition of neurite formation at 150 µg/ml.

The contrasting roles of microglia

Microglia have recently been highlighted as key players in late onset AD, but their exact role remains unclear. There is evidence that microglia have a protective function supported by the link between loss-of-function TREM2 mutations on microglial and AD risk.⁷⁸ There is a growing body of evidence that microglia are directly responsible for neuronal damage in AD. Specifically, microglia have been shown to engulf and remove synapses via a complement-dependent mechanism, and the induction of a microglial pro-inflammatory state may correlate with severity of neurodegeneration.

Initial transcriptomic analysis indicates that varying levels of microglial activation may occur during the course of AD, but more in-depth characterization is needed to confirm this. One hypothesis is that microglial function is normally protective in the brain, with microglia acting as housekeeping phagocytes to maintain tissue homeostasis and keep the extracellular space clean of Aβ.⁷ When Aβ levels rise beyond the ability of microglia to phagocytose and clear these aggregates, microglia compact Aβ aggregates into dense core plaques and shield them off

from neurons, as an attempt to prevent further damage. However, when microglial function becomes inadequate – because of aging or genetic susceptibility – the accumulation of tau aggregates and toxic amyloid plaques induce an inflammatory state in microglia, causing them to eat synapses and secrete neurotoxic cytokines that injure neurons. In this model of disease pathogenesis, microglia have both protective and harmful roles, further complicating analysis of disease progression and the potential of therapeutic approaches targeting microglial activity. This type of complex biological situation is typical of the challenges facing neurodegenerative disease research, and highlights the need for more effective, biologically-relevant model systems that will allow the mechanisms behind disease progression to be investigated effectively.

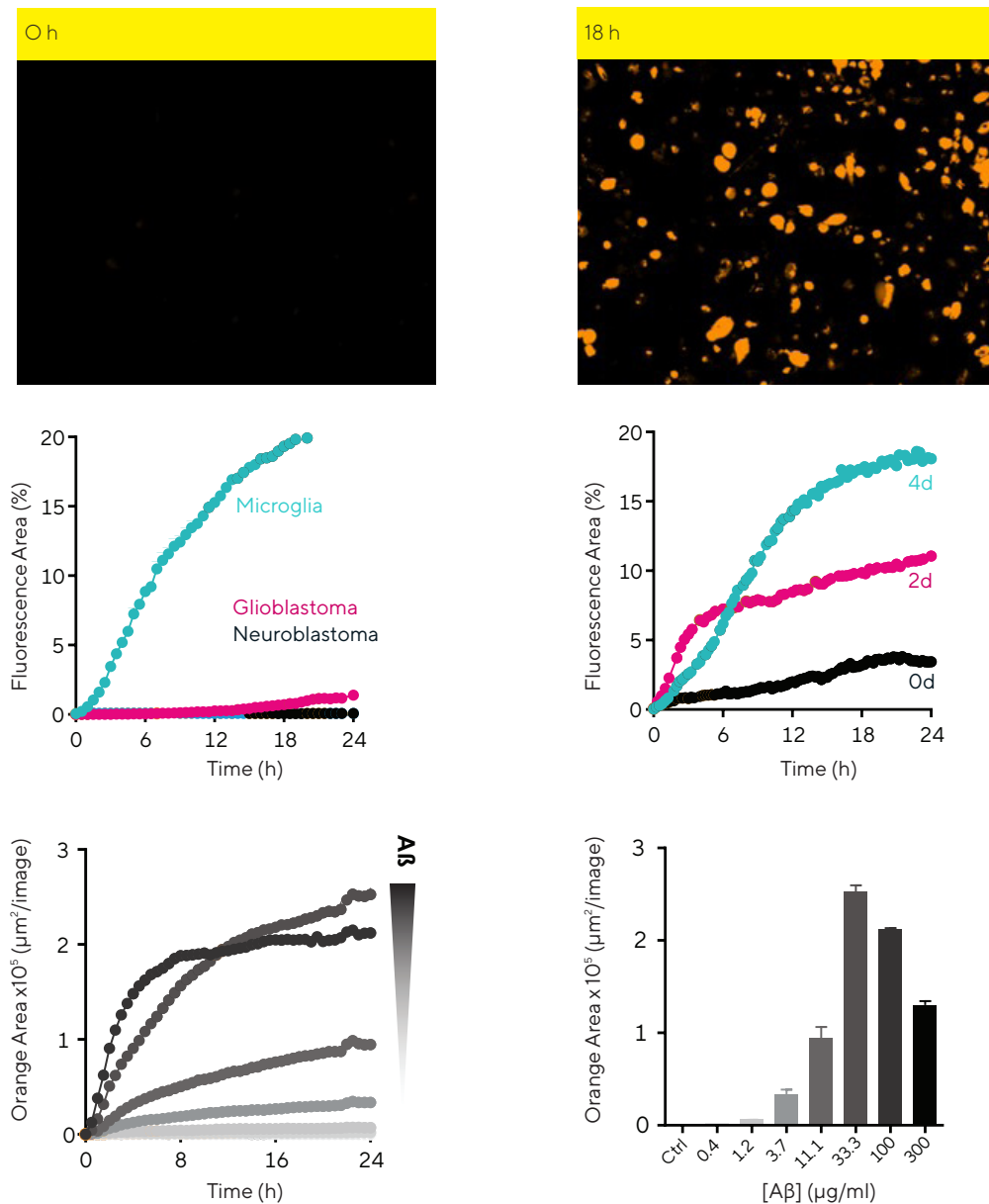


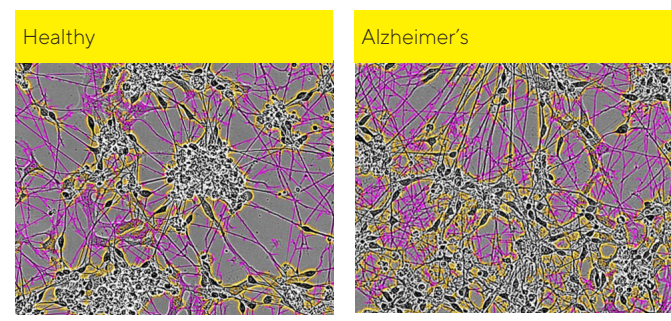
Figure 2: *In vitro* model of phagocytosis of aggregated A β in microglia: hiPSC microglial precursor cells (Axol Bioscience) were seeded into 96-well plates at 30,000 cells/well and differentiated to mature microglia for two weeks. Peptides were labeled using the pHrodo[®] Orange Cell Labeling Kit for Incucyte[®]. Aggregates were formed at 37 °C for 48 hours prior to the assay and added to cells (0.4–300 $\mu\text{g/ml}$). Phase and fluorescent images were acquired in the Incucyte[®] for 36 hours. Representative images compare A β uptake at two time-points. Kinetic time-courses display the cell-type, aggregation and concentration-dependent response to pHrodo-labeled A β peptide over time. Bar chart displays orange area for each concentration at 24 hours.

Creating Cellular Models of AD

Neuroscience traditionally depends on the use of tumor cell lines – such as neuroblastomas or glioblastomas – primary animal or postmortem human tissue. All these approaches are limited in that they do not fully represent the complexity and plasticity of the human brain, limiting the translational value of the models. This lack of biologically-relevant models also makes it difficult to explore the effects of candidate AD therapeutics – a common obstacle to neurological drug development. New methods are therefore required to support and accelerate drug research in this area. Suitable *in vitro* assays, as well as improved analytical approaches, need to be developed to further our understanding of neurodegenerative pathways, and assess the effectiveness of potential therapies for AD.

Advances in induced pluripotent stem cell (iPSC) development offer the potential for easy access to healthy human, patient-, and disease-specific cells, leading to more representative assays and experimental set-ups, thus reducing the reliance on subpar models. Human differentiated neurons from AD patients are now being used to understand more about the disease, and assist in the discovery and evaluation of new drugs.⁹ Thorough characterization of any iPSC-derived model is vital to ensure the reliability and relevance of experimental results. Crucially, the iPSC-based approach also provides a unique opportunity to investigate the molecular variation between AD patients, and develop clinically useful markers for more individualized treatments.

Developing iPSC-based systems to model AD is challenging, due to both the extreme complexity of the microscopic neuroanatomy, and uncertainty regarding key pathogenic steps. AD is primarily characterized by the extracellular deposition of neuritic plaques consisting of misfolded A β peptide, and the intracellular formation of NFTs, accompanied by neuroinflammation and massive neuronal cell and synapse loss at specific brain regions. While it is almost impossible to recreate the whole process *in vitro*, models of AD based on cultured neurons are likely to capture at least some of the key features of early-stage pathology, especially neuronal generation of A β .¹⁰ Despite this, standard neuronal cultures still offer a limited representation of the environment of the central nervous system, and the complex 3D architecture of the brain, making it almost impossible to model the spatial and temporal pathogenic events in 2D culture systems.



Orange: Cell Body Pink: Neurites

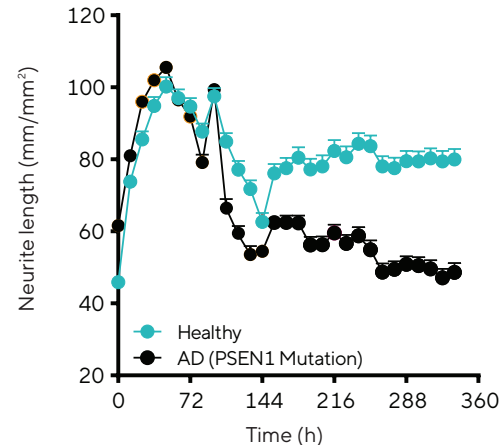


Figure 3: Differential neurite formation from AD patient-derived iPSCs: Healthy and AD (PSEN1 mutation) derived iPSC neurons (Axol Bioscience) were seeded in SureBond+ReadySet-coated 96-well plates at 25,000 cells/well. Neuronal differentiation was induced as per supplier's protocol (supplements A+B). Cultures were placed in the Incucyte® for the duration of the studies. Neurite development was automatically quantified using the Incucyte® Software Analysis Module (Sartorius) for up to 15 days. Time-course showed that the patient-derived AD iPSC line yielded a lower neurite length than the healthy control ($48 \pm 3 \text{ mm/mm}^2$ vs. $80 \pm 3 \text{ mm/mm}^2$ respectively, 3 replicates).

Investigating 2D and 3D Models

Attention has more recently turned to the use of 3D spheroid cultures in an attempt to mimic the brain more closely and to improve *in vitro* modelling of neurological diseases. These spheroids include a variety of neural cell types – neurons, astrocytes and microglia – which can form limited neuronal networks.^{9,10} While in their infancy, these models may be better suited to investigating cell-cell interactions and communication, as well as the effects of pharmacological agents. Combining 3D cell culture techniques with iPSCs derived from AD patients allows the controlled generation of *in vitro* models with many of the key representative features of AD – such as A β aggregation, phosphorylated tau accumulation and neuroinflammatory activity. These new models of AD are invaluable for improving our understanding of AD pathogenesis, and provide a more physiologically-relevant model for testing the efficacy of novel drugs.

The differing behavior and drug-response of cells in 2D and 3D *in vitro* models of AD have been highlighted by a number of research groups. For example, one study using

mass spectrometry to look at A β generation and drug inhibition noted that drug penetration in 3D cultures was significantly lower than in 2D cultures, where drug diffusion is not limited by cellular architecture. This ‘diffusion barrier’ can lead to significant variations in the bioavailability, and therefore efficacy, of the same compound between the two different systems, with much lower responses in 3D neuro-spheroid cultures.⁹ This issue is further compounded by the fact that not all neurons within a 3D environment will be exposed to the same concentration of drug; surface neurons within each spheroid may be exposed to higher drug concentrations than internal cells. Additional research needs to be done in order to understand how this may relate to drug accessibility to different brain regions.

It is also worth noting that intracellular protein trafficking also plays an important role in AD drug response, and neuro-spheroids provide an excellent model to reveal subcellular activities that may be present in the native 3D configurations *in vivo*.

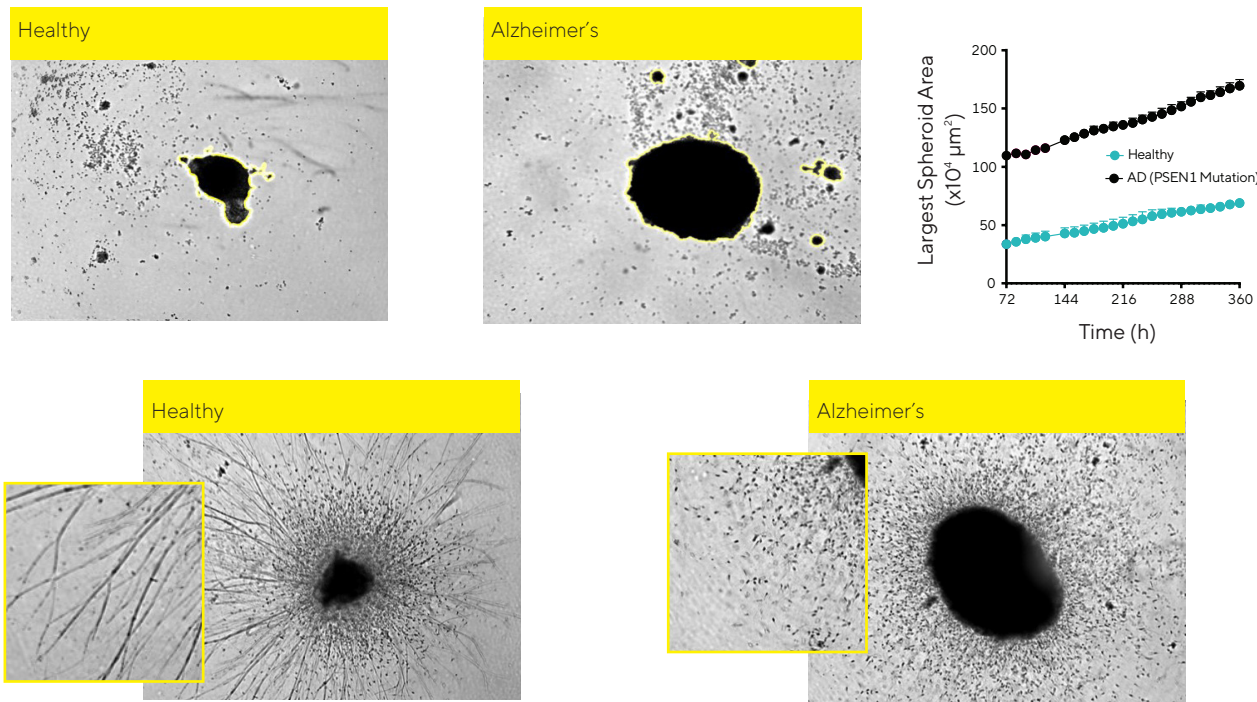


Figure 4: Patient-derived iPSC 3D models reveal distinct spheroid formation and neurite development: Healthy and AD-derived (PSEN1 mutation) iPSC neurons (Axol Bioscience) were plated on ultra-low attachment 96-well plates at 50,000 cells/well, and centrifuged (250 x g for 10 minutes). Single spheroids were allowed to form for 3 days. Cultures were placed in an Incucyte® for the duration of the study. The difference in size was quantified in a non-perturbing manner using brightfield analysis for up to 15 days. Matrigel® (2.25 mg/ml) was added to selected wells at 6 days. Spheroid morphology and process development from the spheroid body was observed for a further 9 days. Time-course showed a distinct spheroid size for both cell lines. Pictures also show the differential process development capability for healthy and Alzheimer's lines.

Current Technology: Advantages and Limitations

Regardless of whether studies are using 2D or 3D cell culture approaches, developing relevant biomarkers, assays and technologies to capture the data that these models can generate is vital. There are a range of cell biology technologies currently used in AD research, with each of them able to offer insights into cellular health, morphology or function.¹¹

Flow cytometry is a widely used and established method for cell-by-cell analysis, where cells are analyzed one at a time using light scattering and fluorescence. Multiple fluorophores and labeled antibodies can be used to perform multivariate analysis of a number of individual parameters in parallel. This approach allows each individual cell to be classified (binned) into a discrete subset, for quantification and characterization – cell health, size, etc. – of each subpopulation.

Similarly, high-content imaging (HCI) methods can be used to determine heterogeneity and perform subset analysis of static cell populations. Typically, nuclear labeling (e.g. with DAPI) is combined with advanced image analysis algorithms to identify individual cell boundaries and identify features on a cell-by-cell basis.

Other methods are widely used to gather functional information by combining electrical (patch clamp¹² or microelectrode array¹³) or chemical (plate reader¹³) information from the cellular cultures. Together, these approaches provide an impressive toolkit for cell-based analysis, but there remains a significant unmet need for additional technical solutions in this area.¹¹ The cell preparation and labeling methods used in the above methods cause significant disruption to the cellular environment, and thus may introduce experimental artifacts. Most of these approaches also only provide a single time-point measure, lacking the ability to track subtle, yet critical changes in cell behavior and function of dynamic cell models. .

A different approach is time-lapse microscopy, where living cells can be observed closely under controlled environmental conditions, typically with single cell tracking and high spatial and temporal resolution. Unlike the other approaches, this gives critical dynamic insight into cell morphology, function and cell/cell interactions, and enables the study of chronic diseases where cells change slowly, such as AD.

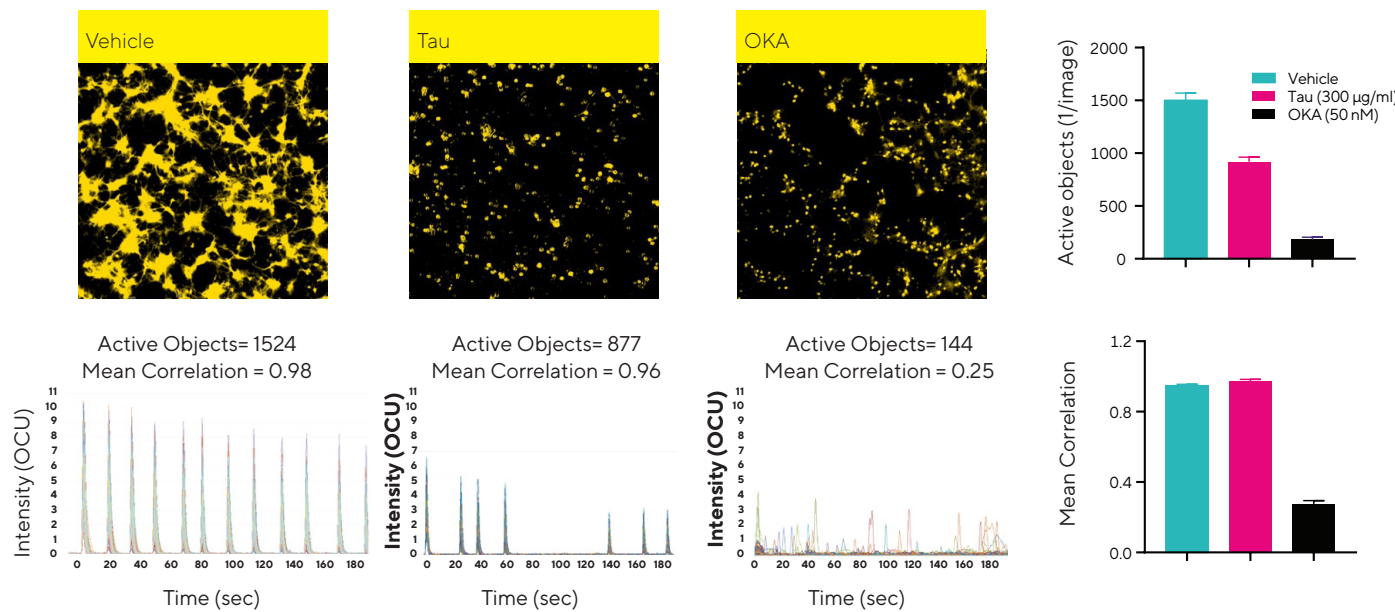


Figure 5: Functional assessment of neuronal activity using time-lapse imaging and analysis: rat cortical neurons and rat astrocytes (Incucyte® rCorticals and rAstrocytes, Sartorius) were seeded as a co-culture (20,000 and 15,000 cells/well respectively) in PDL-coated 96-well plates. Neurons were infected with the genetically-encoded calcium indicator (Incucyte® NeuroBurst Orange Lentivirus, Sartorius) to monitor spontaneous neuronal activity over time through measuring calcium fluctuations. Images were taken every 24 hours in the Incucyte® system (3-minute scans at 3 frames per second). Once mature, functional networks had formed (14 days), cells were treated with either the AD-related peptide tau (aggregated, 300 µg/ml) or the protein phosphatase inhibitor OKA (50 nM). Images show the active range (maximum/minimum fluorescence) over a complete scan. Calcium traces represent calcium fluctuation of all active objects within the field of view. Bar graphs provide the quantification of the number of active objects (1/image) and the correlation (connectivity). This data shows that, compared to vehicle, tau treatment decreased the number of active nodes (1407 ± 94 objects/image vs. 920 ± 43 objects/image) and their mean intensity (13.7 ± 1.7 OCU vs. 7.2 ± 3.6 OCU), while not affecting correlation (0.95 ± 0.01 vs. 0.97 ± 0.01 , 2 replicates). In contrast, OKA decreased the number of active nodes (180 ± 24 objects/image), mean intensity (3.8 ± 0.3 OCU) as well as correlation (0.27 ± 0.02 , 6 replicates) compared to vehicle.

Benefits of Live-cell Analysis

A more recent technological development is the ability to perform live-cell analysis. This approach allows large numbers of cells to be analyzed over long periods of time using non-perturbing cell labeling strategies – potentially opening up valuable new research opportunities for the investigation of AD.

Live-cell analysis allows real-time quantification of the behavior of living cells, by repeatedly acquiring images of the same cells over a time period ranging from hours to weeks or months, with on-the-fly, non-invasive image and data analysis. The technique maintains a stable environment for the cells, so they do not get disrupted during measurements, and can be combined with other analytical technologies – such as those described above – for end-point analyses.¹¹

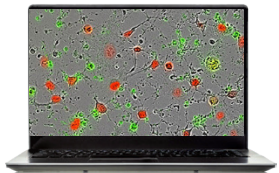
Purpose-built live-cell analysis systems like the Incucyte® (Sartorius) provide a fast, flexible and powerful solution for continuous live-cell analysis, combining image acquisition, processing and data visualization using a suite of non-perturbing cell labeling and reporter reagents. The Incucyte's advanced analysis platform resides within a standard cell incubator, allowing automated imaging and two-color fluorescence analysis while maintaining full environmental control. Crucially, the optical path moves, rather than the culture plate, so that the cells are not disturbed during image capture. This allows researchers to easily observe and analyze defined subsets of living cells over time – based on morphological, surface markers, cell health and/or functional properties – for up to 6 microplates in parallel.



Incucyte® SX5 Live-Cell Analysis System

System

A fully automated image and analysis system that resides within a standard cell incubator for optimal cell viability. Leverage up to five total fluorescence channels (up to three simultaneously) for long term time-lapse experiments, including a long wavelength, low phototoxicity NIR channel.



Incucyte® Software

Fast, flexible and powerful control hub for continuous live-cell analysis comprising image acquisition, processing and data visualization.



Incucyte® Reagents and

Consumables

A suite of non-perturbing cell labeling and reporter reagents. Includes novel, non-perturbing fluorescent reagents for neurite outgrowth and neuronal activity, plus no-wash cell health reagents for apoptosis and cytotoxicity.

Summary

The pathogenesis of AD and other neurodegenerative diseases is clearly highly complex, with seemingly conflicting datasets regularly being reported in the literature. The reasons for this are likely to be multifaceted, but the inherent weakness of animal models and traditional experimental approaches no doubt contributes to this lack of clarity. It is now better accepted that iPSC-derived disease models offer more biologically-relevant results than standard preclinical approaches, and that a combination of 2D and 3D cell culture technologies will be required to accelerate the development of new therapies.

The study of chronic, progressive diseases requires technologies – such as live-cell analysis – that are capable of following dynamic cellular processes under stable, controlled conditions. Managing and analyzing the large quantities of data that these systems generate over the course of experiments that last weeks, or even months, will be the next big challenge. Here, advanced analytics such as artificial intelligence may have a role to play, allowing the processing of vast, complex datasets to reveal previously unrecognized insights. This novel approach, combining long-term, continuous monitoring of relevant live-cell models with integrated analysis is likely to yield significant breakthroughs, and could be the answer to drug discovery for chronic illnesses.

References

1. Wyss-Coray T, Rogers J. Inflammation in Alzheimer disease—A brief review of the basic science and clinical literature. *Cold Spring Harb Perspect Med*, 2(1):a006346 (2012).
2. Hebert LE, Weuve J, Scherr PA, Evans DA. Alzheimer disease in the United States (2010–2050) estimated using the 2010 Census. *Neurology*, 80(19):1778–83 (2013).
3. Hurd MD, Martorell P, Delavande A, Mullen KJ, Langa KM. Monetary costs of dementia in the United States. *N Engl J Med*, 368:1326–34 (2013).
4. Alzheimer A. Über eine eigenartige Erkrankung der Hirnrinde. *Allgemeine Z Psychiatrie Psychisch. Gerichtliche Med*, 64:146–8. (1907).
5. Ballatore C, Lee V, Trojanowski J. Tau-mediated neurodegeneration in Alzheimer's disease and related disorders. *Nat Rev Neurosci*, 8(9):663–72 (2007).
6. Verheyen A, Diels A, Dijkmans J, Oyelami T, Meneghelli G, Mertens L, Versweyveld S, Borgers M, Buist A, Peeters P, Cik M. Using Human iPSC-Derived Neurons to Model TAU Aggregation. *PLoS One*, 10(12);p. e0146127 (2015).
7. Hansen DV, Hanson JE, Sheng M. Microglia in Alzheimer's disease. *J Cell Biol*, 217(2):459–72 (2018).
8. Ransohoff R. How neuroinflammation contributes to neurodegeneration. *Science*, 353(6301):777–83 (2016).
9. Lee HK, Velazquez Sanchez C, Chen M, Morin PJ, Wells JM, Hanlon EB, Xia W. Three Dimensional Human Neuro-Spheroid Model of Alzheimer's Disease Based on Differentiated Induced Pluripotent Stem Cells. *PLoS One*, 11(9);e0163072 (2016).
10. Park J, Wetzel I, Marriott I, Dréau D, D'Avanzo C, Kim DY, Tanzi RE, Cho H. A 3D human triculture system modeling neurodegeneration and neuroinflammation in Alzheimer's disease. *Nat Neurosci*, 21:941–51 (2018).
11. Essenbioscience.com. White Paper: Live-cell analysis of cell subsets and Heterogeneity. [online] Available at: <https://www.essenbioscience.com/en/communications/white-paper-cell-subsets-and-heterogeneity/> (2020) [Accessed 12 Feb. 2020].
12. Daily N, Du Z, Wakatsuki, T. High-Throughput Phenotyping of Human Induced Pluripotent Stem Cell-Derived Cardiomyocytes and Neurons Using Electric Field Stimulation and High-Speed Fluorescence Imaging. *ASSAY DRUG DEV TECHN*, 15(4):178–88 (2017).
13. Bar El Y, Kanner S, Barzilai A, Hanein Y. Calcium imaging, MEA recordings, and immunostaining images dataset of neuron-astrocyte networks in culture under the effect of norepinephrine. *Gigascience*, 8(2) (2018).

Keywords or phrases:

Research Use Only (RUO), Cytokines, Growth Factors, Neuronal Differentiation, Live-Cell Analysis, Live-Cell Immunocytochemistry (ICC), Neurite Outgrowth, Neurotrack

Optimization of SH-SY5Y Differentiation Using Growth Factors and Cytokines

Jasmine Trigg, Daryl Cole, Natasha Lewis, Nicola Bevan, Tim Dale

Sartorius UK Ltd, Units 2 & 3 The Quadrant, Newark Close, Royston, Hertfordshire, SG8 5HL, UK

Correspondence
E-Mail: AskAScientist@sartorius.com

Introduction

For neuroscientific research a crucial component is utilizing appropriate model systems which are translational for studying human development and disease. The use of *in vitro* models has greatly enhanced the field and traditionally these include primary rodent neuronal cultures, end-point slice cultures, and immortalized cell lines.¹ Growth factors and cytokines are signaling molecules that play critical roles in these models and are involved in a wide range of functions including cell growth, differentiation, and survival.^{2,3}

SH-SY5Y cells, which exist as two morphologically distinct phenotypes including epithelial-like (S-type) or neuroblast-like (N-type), are a subclone of the human SK-N-H parental neuroblastoma cell line.^{4,5} They are a widely used *in vitro* model as they can be differentiated into a neuronal-like phenotype. Additionally, unlike primary rodent or induced pluripotent stem cell (iPSC)-derived neurons, they afford the benefit of being open to low-cost large-scale expansion, amenable to genetic modification, and express human-specific proteins.^{6,7} SH-SY5Y cells can be differentiated through several different mechanisms depending on the phenotype of interest including all-trans retinoic acid (atRA)⁸,

phorbol esters⁹, and neurotrophic factors such as insulin-like growth factor 1 (IGF-1)¹⁰, brain-derived neurotrophic factor (BDNF)¹¹, and bone morphogenic protein 4 (BMP-4)¹². Typically, upon differentiation into a neuronal-like phenotype, these cells cease proliferating, develop neurite-like extensions, form functional synapses, and express mature neuronal markers such as microtubule associated protein (MAP) and neural cell adhesion molecule (NCAM or CD56).^{11,13}

Currently, these protocols are not well-defined and can induce variable and heterogenous populations of neurons.¹ Moreover, standard approaches to studying neuronal differentiation rely on end-point assays including high-content analysis, fixed immunocytochemistry (ICC), or flow cytometry. These often require destructive protocols preventing visual assessment of morphological changes and provide limited kinetic information. To successfully use these *in vitro* models across a variety of neuroscientific research areas, approaches to reproducibly generate homogeneous neuronal cultures and technology pipelines to visualize and temporally quantify these complex models are required.

In this application note, we demonstrate robust differentiation of human SH-SY5Y cells into neuronal-like cells using Sartorius Research Use Only (RUO) Growth Factors and Cytokines and the utility of Incucyte® Live-Cell Imaging and Analysis to kinetically visualize and quantify changes in proliferation, morphology, and cell surface antigen expression.

Assay Principle

Sartorius offers a range of high-quality human RUO Growth Factors and Cytokines that are produced using recombinant DNA technology and do not contain any animal-derived components. These growth factors are of high-purity, low endotoxicity, and can be used for the long-term differentiation or maintenance of neuronal cultures in a non-perturbing and reproducible manner.

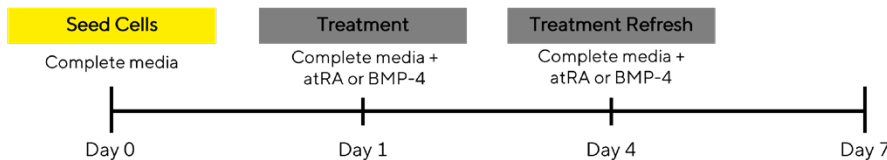
The Incucyte® Live-Cell Analysis System enables kinetic monitoring and quantification of cell cultures using HD Phase-contrast and fluorescence images, which are automatically quantified via integrated software. Purpose-built Incucyte® Neurotrack Analysis Software enables the quantification of neuronal outgrowth to be measured in mono-cultures label-free without perturbing sensitive cultures. Additional insights can be gained using Incucyte® Fabfluor Antibody Labeling Dyes, which, once complexed to Fc containing antibodies of interest, enable dynamic monitoring of surface antigen expression in live cells. Importantly, these combined approaches enable multiparametric analyses of cell morphology and phenotype and the temporal association of these with neuronal differentiation.

Materials and Methods

SH-SY5Y human neuroblastoma cells were stably transfected with Incucyte® NuLight Orange Lentivirus, a nuclear restricted fluorescent marker. Undifferentiated SH-SY5Y cells were cultured in DMEM/F12K (1:1) supplemented with 10% fetal bovine serum (FBS) and 1% Pen/Strep (complete media).

For differentiation, SH-SY5Y cells were seeded into 96-well TPP plates (Cat. No. 92096) and allowed to adhere until a confluence of ~15% was achieved. As outlined in Figure 1, we used two methods for SH-SY5Y differentiation into neuronal-like phenotypes. These utilized atRA (10 μ M) and/or Sartorius RUO Recombinant Human Growth Factors or Cytokines including BMP-4 (Cat. No. CYK-0025-0006) and BDNF (Cat. No. CYK-0100-0008). Sartorius RUO Glia-Derived Neurotrophic Factor (GDNF; Cat. No. CYK-0025-0009) and Neurotrophin-3 (NT-3; CYK-0025-0020) were also used in optimization studies. Cultures were monitored in an Incucyte® Live-Cell Analysis System at 2 – 4 hour intervals for up to 14 days. Media refreshes were performed every 2 – 3 days.

Method 1: atRA or BMP-4 differentiation



Method 2: atRA+ BDNF Gradual Serum Starvation

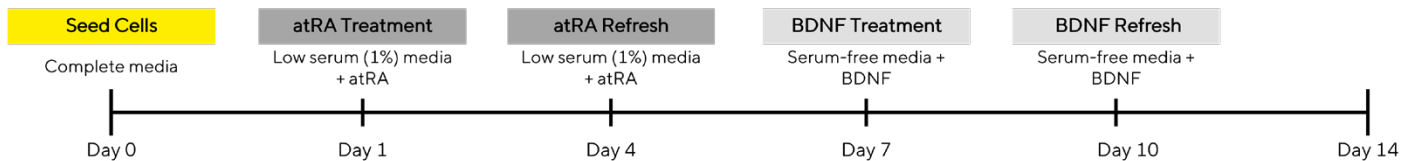


Figure 1. Schematic of methods for neuronal differentiation. Methods outlined for differentiating human SH-SY5Y neuroblastoma cells into neuronal-like phenotypes. These utilize Sartorius RUO Growth Factors and Cytokines and the Incucyte® Live-Cell Analysis System to enable image-based measurements of differentiation in real-time.

The Incucyte® Live-Cell immunocytochemistry (ICC) assay involves a simple mix-and-read, no wash protocol in a 96/384-well format as demonstrated in Figure 2. Once labeled with isotype matched Incucyte® IgG1 Fabfluor-488 (Cat. No. 4745) or IgG2a Fabfluor-488 (Cat. No. 4743)

Labeling Dyes, the Fabfluor-antibody complex in combination with Incucyte® Opti-Green background suppressor was added to live-cells. Azide-free antibodies of interest were used to minimize perturbation to long-term sensitive cultures.

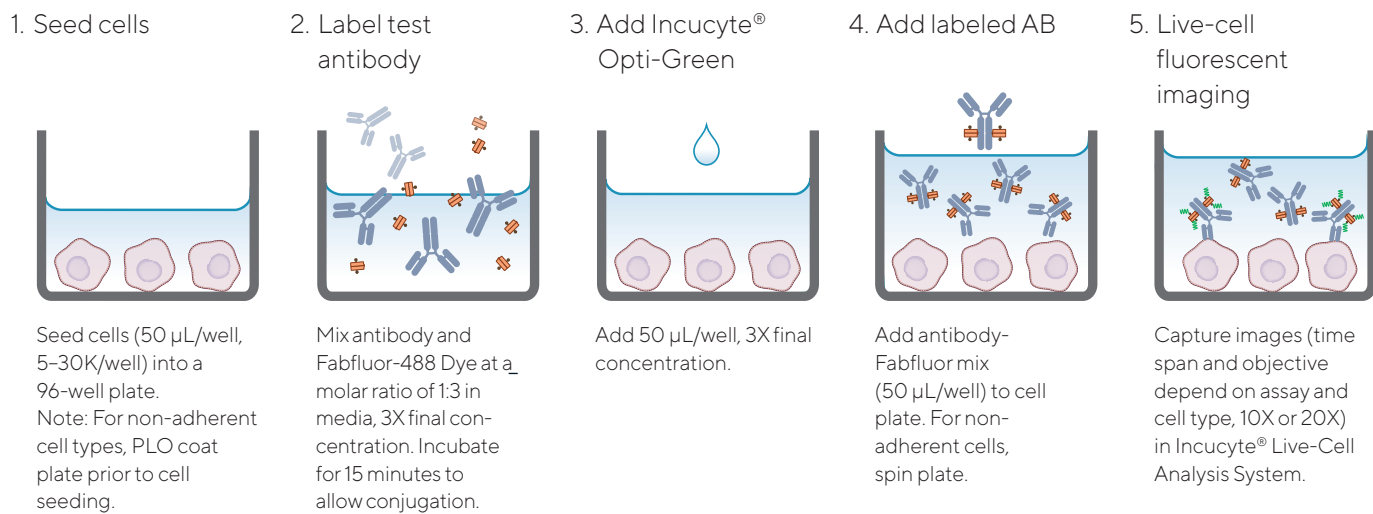


Figure 2. Quick guide of Incucyte® Live-Cell Immunocytochemistry (ICC) protocol. The simple mix-and-read protocol utilizes Incucyte® Fabfluor Antibody Labeling Dyes and the Incucyte® Live-Cell Analysis System for image-based fluorescent measurements of surface antigen expression.

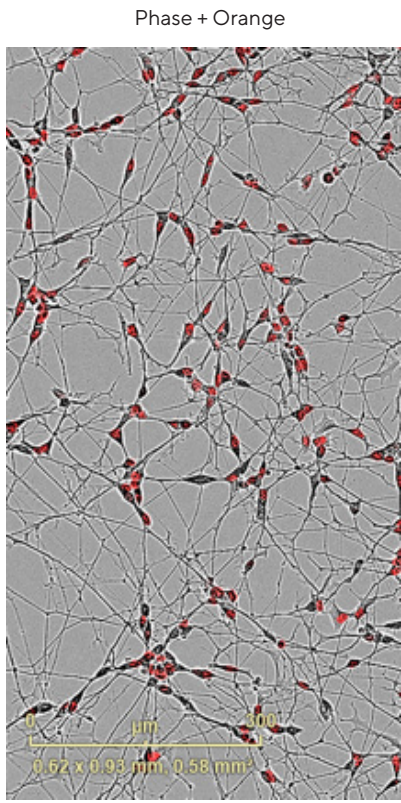
Quantification of Dynamic Changes During Neuronal Differentiation

The Incucyte® Neurotrack Analysis Software Module automatically segments phase images and generates metrics describing neurite length, neurite branching, and cell-body clusters (count or area). Additional nuclear count measurements can be obtained when cells contain a fluorescent nuclear label. Here we demonstrate how this software can be used to quantify cell proliferation and morphological changes, such as neuronal outgrowth, as indicators of neuronal differentiation (Figure 3). SH-SY5Y cells stably expressing Incucyte® NuLight Orange were differentiated using a gradual serum-starvation method with the sequential introduction of atRA (10 μ M) and BDNF (50 ng/mL) (method 1). Representative phase and fluorescence images (Figure 3A) for differentiated SH-SY5Y cells reveal a mature neuronal-like phenotype with reduced cell body size and extended neurites on day 14. The segmentation masking of fluorescent cell nuclei or label-free segmentation of neurites and cell-body clusters

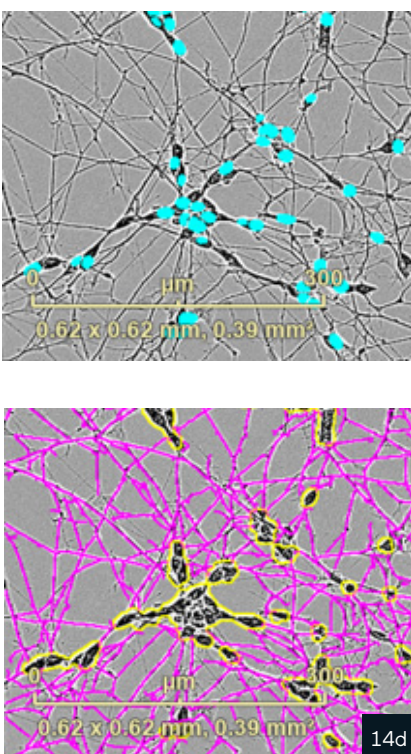
are also shown. The resulting quantification revealed that proliferation is inhibited over-time for differentiated compared to undifferentiated cells (Figure 3B) and we observed a kinetic increase in neurite length following BDNF addition compared to serum-free control (Figure 3C).

The Incucyte® Live-Cell ICC Assay permits dynamic quantification of cell surface antigen expression. Automated imaging and integrated analysis tools enable image-based measurements of fluorescence over the entire assay time course and, alongside Opti-Green, minimize background fluorescence. In the absence of expressed specific antigen, little-to-no signal is observed on the cells. Cell surface expression can be quantified using several metrics, including fluorescence area (Total Green Object Area), fluorescence intensity integrated over the area of detectable fluorescence (Total Green Object Integrated Intensity), or through normalizing the fluorescence area to cell coverage (Green Object Confluence/Phase Confluence).

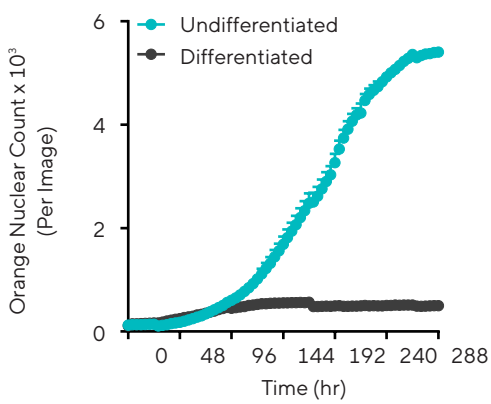
A.



Phase + Masks



B.



C.

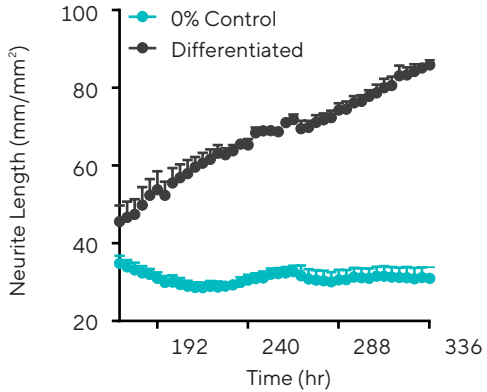


Figure 3. Visualization and quantification of neuronal differentiation. SH-SY5Y-NuLight Orange cells were differentiated by gradual serum starvation (10 – 0%) in combination with atRA (10 μ M) and Sartorius Recombinant Human BDNF (50 ng/mL). Images were acquired at 10X over 14 days using the Incucyte® Live-Cell Analysis System and quantified using integrated Incucyte® Neurotrack Analysis Software. A) Representative phase and fluorescence images and segmentation masks of fluorescence cell nuclei (blue), label-free neurites (pink) and cell-body clusters (yellow outline) shown at 14 days. B) Time courses display change in orange nuclear count and neurite length. Data presented as mean \pm SEM, n = 3 replicates.

A.

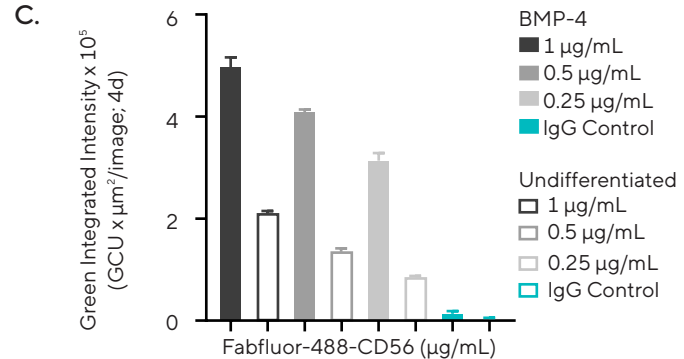
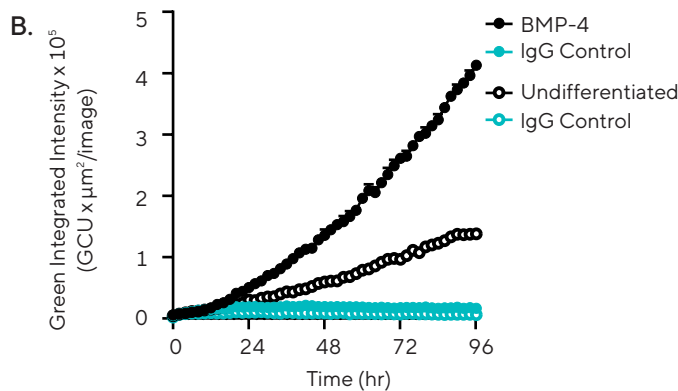
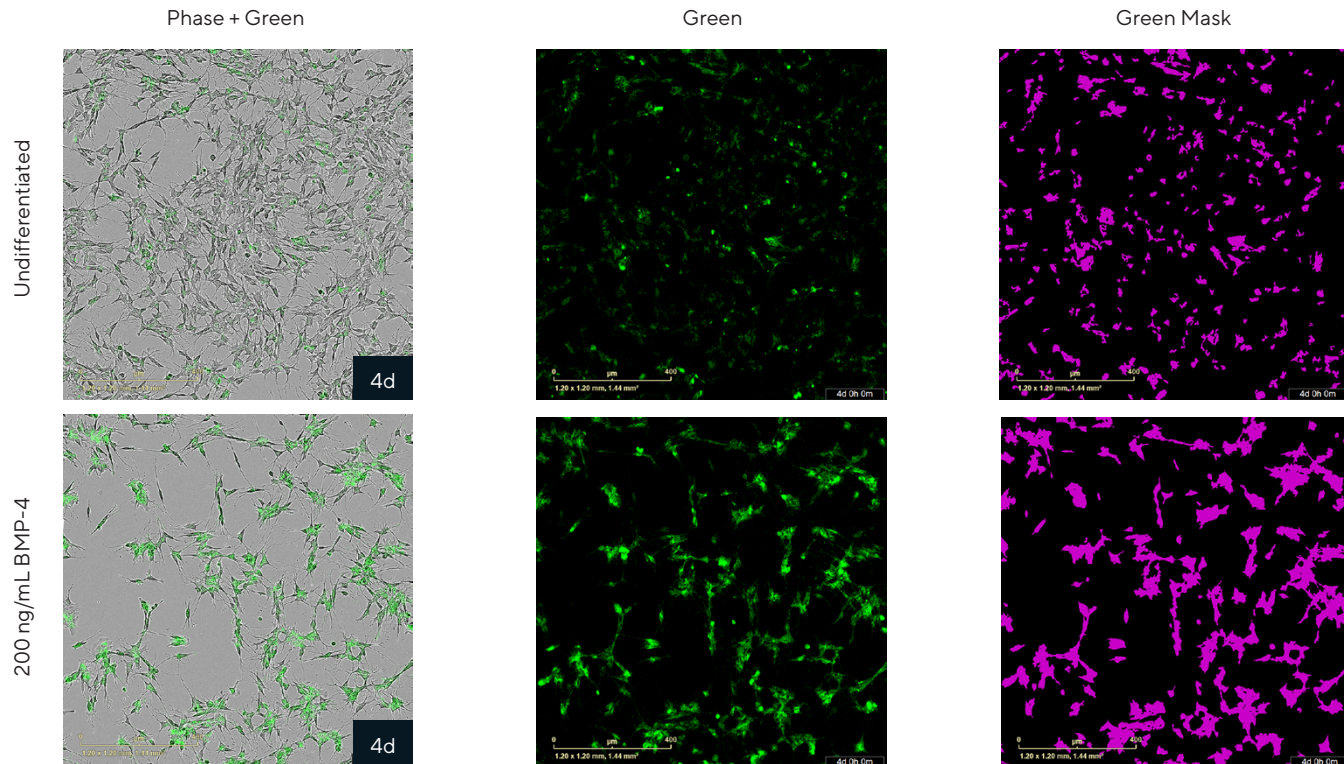


Figure 4. Live-cell immunochemistry (ICC) labeling optimization using BMP-4 model of differentiation. SH-SY5Y-NuLight Orange cells were treated with a concentration range of Fabfluor-488-CD56 antibody complexes (0.25 – 1 μ g/mL) in the presence of Opti-Green under undifferentiated or BMP-4 (200 ng/mL) differentiated conditions. A) Representative phase and fluorescence images for undifferentiated and differentiated cells on day 4 with Fabfluor-488-CD56 shown in green and segmentation mask in magenta. B) Time course for Total Green Integrated Intensity over 4 days for 0.5 μ g/mL Fabfluor-488-CD56 or IgG isotype control in undifferentiated or differentiated conditions. C) Total Green Integrated Intensity on day 4 shown for all conditions. Data presented as mean \pm SEM, n = 3 replicates.

To exemplify quantification of changes in CD56 surface antigen expression during BMP-4 differentiation we optimized live-cell ICC labeling using a concentration range of Fabfluor-488-CD56 antibody complexes (Figure 4). Shown are representative images and the segmentation mask used (Figure 4A). Quantification of the green integrated intensity, which accounts for both changes in green intensity and cell area, showed that undifferentiated cells have a basal level of CD56 expression which kinetically increases with BMP-4 differentiation (Figure 4B). This increase in CD56 expression was antibody-complex concentration-dependent across both conditions, whilst

little-to-no fluorescence was detected for IgG isotype controls (Figure 4C). To determine an optimal antibody-complex concentration, we assessed the assay windows between undifferentiated and differentiated conditions and directly confirmed that we could visualize and quantify fluorescence in both the cell body and neurite-like extensions. We selected 0.5 μ g/mL for use in subsequent experiments as it provided a good assay window and the desired distribution of fluorescence. Overall, these methods can robustly be used to quantify the dynamic changes that occur with neuronal differentiation.

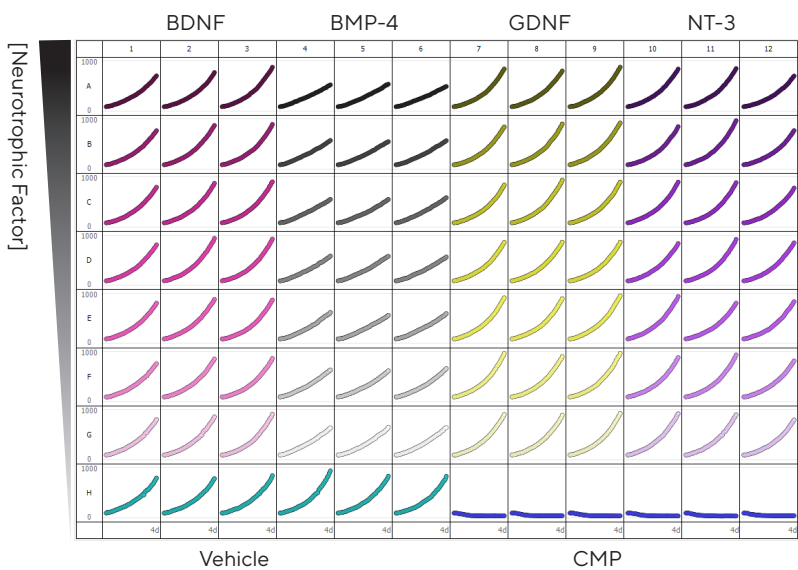
Growth Factor and Cytokine Concentration Assessment

To optimize concentrations of differentiation-inducing treatments, SH-SY5Y-Nuclight Orange cells were treated with a concentration range of four Sartorius Growth Factors and Cytokines including BDNF, BMP-4, GDNF, and NT-3, and monitored using the Incucyte® Live-Cell Analysis System (Figure 5). The microplate view reports orange nuclear count normalized to pre-treatment over 4 days (Figure 5A) and we observed no toxicity for all neurotrophic factors at the concentrations studied compared to positive

control camptothecin (CMP). BMP-4 induced modest inhibition on cell proliferation across all concentrations compared to vehicle (Figure 5B). HD images also confirmed subtle morphological changes in BMP-4 treated cells with the development of neurite-like extensions, consistent with known differentiating effects.¹² The data demonstrates the ability to accurately monitor cell viability in a 96-well throughput and highlights the reproducibility of Sartorius RUO Growth Factors and Cytokines.

A.

Orange Count %
Normalized to pre-treatment



B.



C.

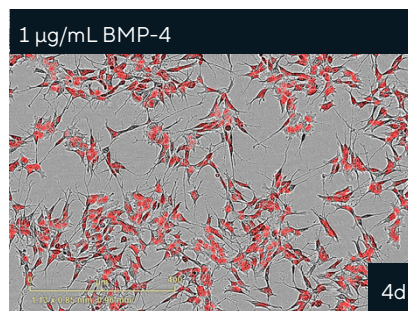


Figure 5. Neurotrophic factor concentration range assessment. SH-SY5Y Nuclight Orange cells were treated with neurotrophic factors BDNF, BMP-4, GDNF, and NT-3 (1 – 0.01 µg/mL) and monitored using the Incucyte® Live-Cell Analysis System. 10 µM Camptothecin (CMP) was used as a positive control for cell death. A) Microplate graph shows nuclear count normalized to pre-treatment over 4 days for all treatment conditions. B) Blended phase and orange images shown at 4 days for 1 µg/mL BMP-4 and vehicle (10X). Data shown as mean ± SEM, n = 3 – 6 replicates.

Monitoring Proliferation and Cell Surface Antigen Expression during BMP-4 differentiation

RA is a Vitamin A derivative commonly used to inhibit cell growth and rapidly differentiate SH-SY5Y cells from a N-type to a neuronal-like phenotype. However, studies suggest that RA does not strongly promote neuronal marker expression and long-term treatment results in heterogeneous populations due to transdifferentiation occurring between N- and S-types.^{14,11} To avoid these limitations, and obtain higher-quality neuronal cultures, different approaches are increasingly being applied. One approach is the use of BMP-4, a signaling molecule that is part of Transforming growth factor-beta (TGF- β) protein superfamily.¹⁵ BMP-4 appears to play crucial roles in neural stem cell development, axonal growth, and has been shown to promote neuroblastoma differentiation.^{16,17}

We previously established that BMP-4 induced morphological changes in SH-SY5Y cells consistent with a neuronal-like phenotype (Figure 5). Subsequently, we investigated any associated changes in surface antigen expression through kinetically examining CD24, a N-type neural precursor marker highly expressed in

undifferentiated cells, and the neuronal marker CD56.^{18,12} SH-SY5Y Nuclight Orange Cells were treated with atRA or a concentration range of BMP-4 in the presence of Incucyte® Fabfluor-488 Dye complexed to CD24, CD56, or isotype controls (Figure 6). Fluorescence images indicated changes in nuclear count, and expression and distribution of CD56 for BMP-4 compared to atRA and undifferentiated cells (Figure 6A). Quantification showed BMP-4 induced a concentration-dependent inhibitory effect on proliferation compared to control over 5 days with maximal inhibition being slightly lower than that observed for atRA (2.26 ± 0.3 , 1.56 ± 0.1 , $4.99 \pm 0.4 \times 10^3$ count per image, for BMP-4, atRA, or control, respectively) (Figure 6B). For CD24 we observed a marked decrease for atRA and a modest concentration-dependent decrease for BMP-4 suggesting partial loss of neural precursor expression (Figure 6C). In contrast, for CD56 we observed a slight increase in expression for atRA and an enhanced concentration-dependent increase for BMP-4 (EC_{50} value of 4.72 ng/mL , 95% CI [3.65, 6.20] (Figure 6D)). Overall, these data confirm that BMP-4 differentiation induces homogenous neuronal-like phenotypes and highlights how this approach facilitates insights into neuronal differentiation and cellular interconversion.

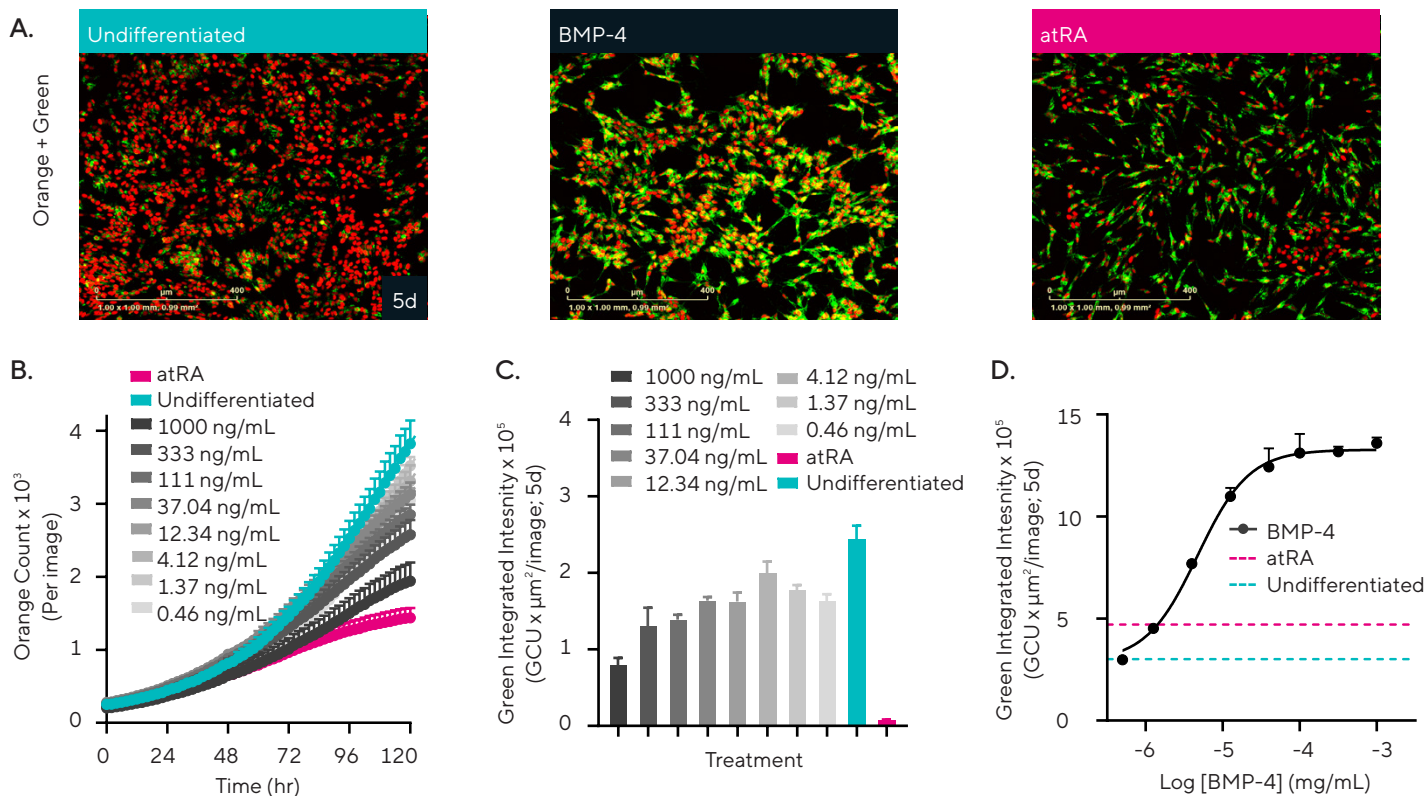


Figure 6. BMP-4 differentiation induces concentration-dependent changes in proliferation and surface antigen expression. SH-SY5Y Nuclight Orange cells were differentiated with BMP-4 (1000 – 0.41 ng/mL) or atRA (10 μM) and treated with either Incucyte® Fabfluor-488 antibody complexed to CD24, CD56, or IgG control. A) Representative Green and Orange blended fluorescence images shown for undifferentiated, BMP-4 (1000 ng/mL) or atRA differentiated cells at 5 days. B) Time course shown for orange nuclear count over 5 days. C) Total Green Integrated Intensity shown for CD56 at 5 days. D) Transformed data shows concentration response curve to BMP-4 for CD56 expression at 5 days; vehicle (teal) and atRA (magenta) plotted as dashed lines. Data presented as mean \pm SEM, $n = 3$ replicates.

Kinetic Assessment of BDNF Differentiation

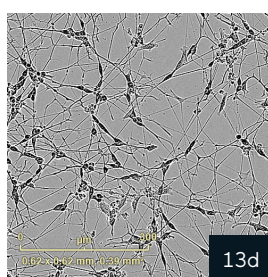
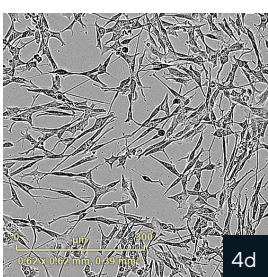
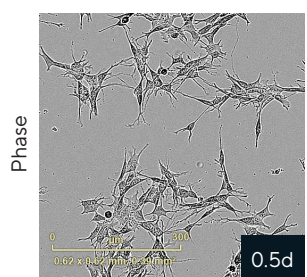
BDNF protein, a member of the neurotrophin family, plays essential roles in the regulation of neuronal development, including differentiation, axonal growth, synapse formation, maturation, and maintenance.^{19,20} It is used across several *in vitro* applications, including the differentiation of neural progenitor cells, cortical organoids, and immortalized human cell lines.^{21,22}

One established protocol for the differentiation of SH-SY5Y cells to a neuronal-like phenotype is based on gradual removal of serum from the media and sequential treatments with atRA and BDNF.¹¹ This method has been shown to augment the differentiating properties of atRA and generate homogeneous populations of cells with enhanced neuronal-like characteristics, including a more mature morphology, elevated neuronal marker expression, and improved cell survival.^{11,23,24} To assess this method and examine the effects of BDNF, SH-SY5Y-Nuclight Orange cells were differentiated using a gradual serum-starvation method with the addition of atRA (10 μ M) followed by a concentration-range of BDNF (method 2). Differentiation

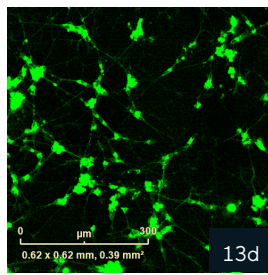
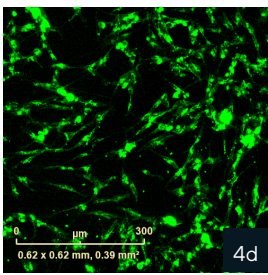
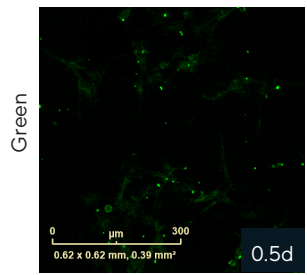
was performed in the presence of Incucyte[®] Fabfluor-488 Dye complexed to CD56, housekeeping marker CD71, or IgG isotype control.

Phase images reveal the temporal morphological changes occurring during differentiation using this method (Figure 7A). In undifferentiated form, SH-SY5Y neuroblast-like cells are non-polarized with few truncated processes; during the initial stages of atRA differentiation cells elongate and form neurite-like extensions. In later stages with BDNF, the cell bodies retract and form clusters with neurites developing extensive, branched networks similar to primary or iPSC-derived neurons. Green fluorescence images show the corresponding CD56 expression (Figure 7B). The results revealed temporal changes in neuronal-specific CD56 expression throughout the differentiation process (Figure 7C), with a rapid increase observed initially and more subtle changes in intensity and distribution observed at later time points. Little-to-no expression was observed for IgG control and CD71 showed stable and homogeneous expression throughout. Additionally, we observed concentration-dependent differences in CD56 expression, with a bell-shaped response to BDNF at 14 days (Figure 7D).

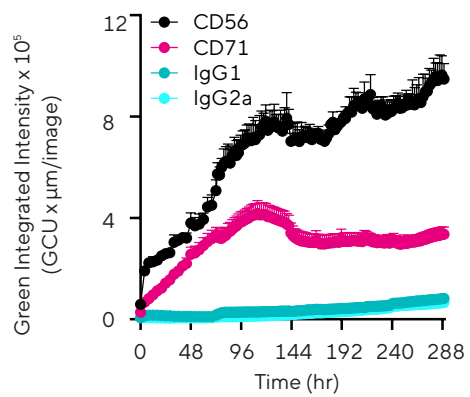
A.



B.



C.



D.

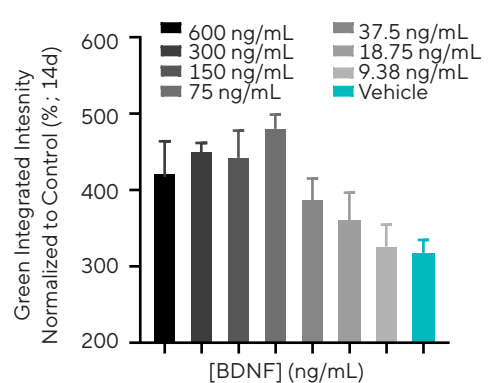


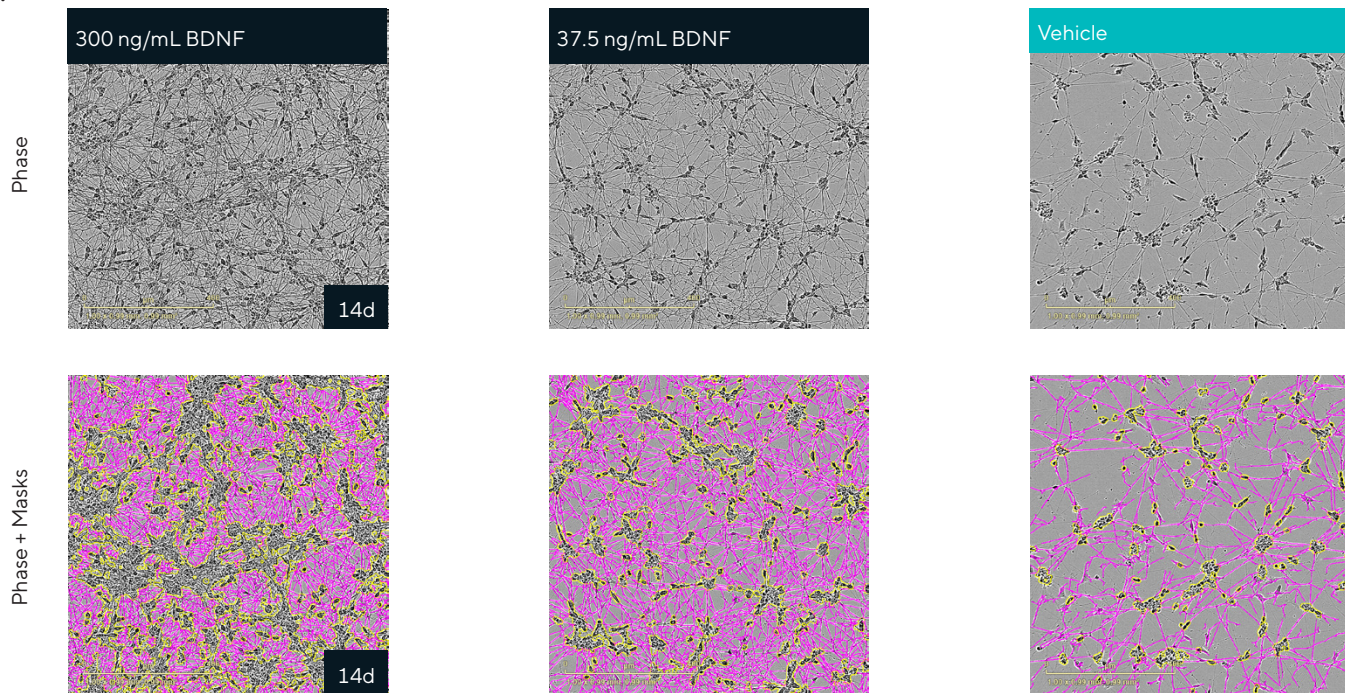
Figure 7. Kinetic monitoring of cell surface antigen expression during SH-SY5Y differentiation into a mature neuronal-like phenotype. SH-SY5Y Nuclight Orange cells were differentiated by gradual serum starvation (10 – 0%) in combination with atRA (10 μ M) and a concentration-range of Sartorius Human Recombinant BDNF (600 – 9.38 ng/mL) for up to 14 days. Differentiation was performed in the presence of Incucyte[®] Fabfluor-488 antibody complexed to CD56 (neuronal marker), CD71 (housekeeping protein), or IgG control and Opti-Green. Timelapse Phase (A) and fluorescence images (B) shown for differentiation using atRA and 50 ng/mL BDNF. C) Time course of Green Integrated Intensity shown for all conditions. D) Bar graph shows CD56 expression in response to BDNF or vehicle control at 14 days. Green integrated intensity was normalized to IgG control to account for some observed autofluorescence of clustered cell bodies in mature cultures. Data presented as mean \pm SEM, $n = 3 - 5$ replicates.

Additionally, we quantified morphological changes using Incucyte® Neurotrack Analysis Software. Shown are HD phase contrast images for differentiated SH-SY5Y cells and the label-free segmentation used to mask neurites and cell body clusters (Figure 8A). We observed a mature homogeneous neuronal-like phenotype with morphological differences detected at different concentrations of BDNF compared to vehicle (serum-free media). Transformation of the data showed BDNF induced a concentration-dependent effect on neurite development, including neurite length, branch points, and cell-body cluster area (Figure 8B). Notably, the absence of BDNF results in cellular apoptosis as visualized in the vehicle images. This is suggestive of differentiated SH-SY5Y survival

being dependent on BDNF in serum-free conditions and consistent with BDNF being a known regulator of cell survival in neuronal cultures.¹¹

Overall, these data confirm that this method reproducibly induces temporal changes in morphology and surface antigen expression consistent with neuronal differentiation, with the commonly used concentration of 50 ng/mL BDNF proving to be within an optimal range. The data also highlights the amenability of this multiplexed approach to optimize long-term differentiation protocols in a 96-well microplate throughput using high-quality RUO Growth Factors and Cytokines.

A.



B.

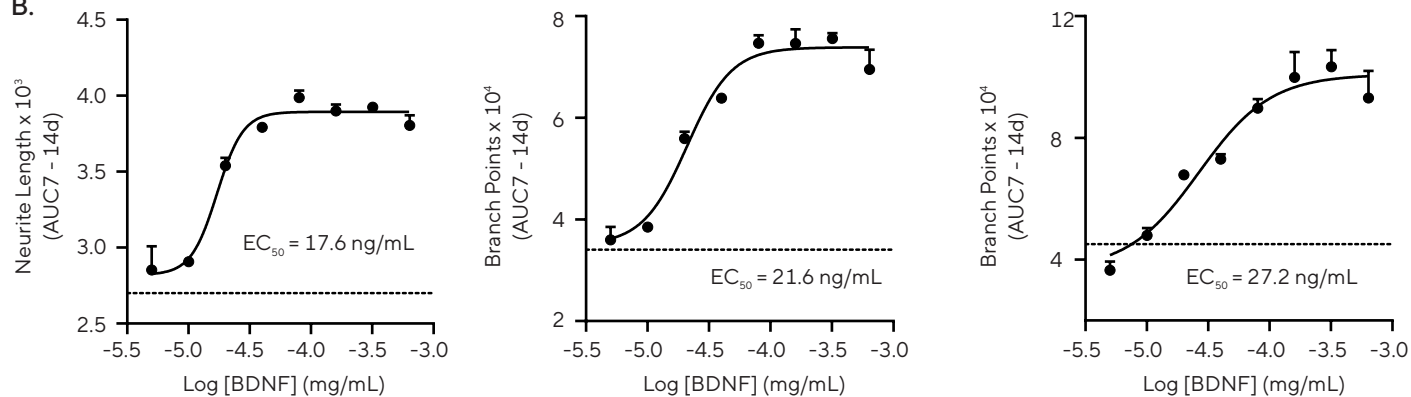


Figure 8. Concentration-dependent neurite development in response to BDNF. SH-SY5Y cells were differentiated by gradual serum starvation (10–0%) in combination with atRA (10 μ M) and a concentration range of Human Recombinant BDNF (600–4.69 ng/mL). Images were acquired at 10X over 14 days using the Incucyte® Live-Cell Analysis System and quantified using integrated Incucyte® Neurotrack Analysis Software. A) HD Phase images for BDNF differentiated neuronal cultures compared to serum-free vehicle control. Label-free segmentation masks of neurites (magenta) and cell-body clusters (yellow outline) also shown. C) Concentration response curves of Neurotrack morphological readouts showing Neurite Length, Neurite Branch Points, and Cell-Body Cluster Area (AUC 7–14 days). Data presented as mean \pm SEM, n = 3 replicates.

Summary and Outlook

Brain development and differentiation are highly sophisticated, dynamic processes involving a complex interplay of several growth factors and cytokines, which require robust, translational *in vitro* models that accurately recapitulate desired phenotypes. The data shown demonstrates how utilizing Sartorius RUO Growth Factors and Cytokines in combination with live-cell analysis methods is a powerful approach for reproducibly generating *in vitro* neuronal cultures. This approach facilitates optimization of cell culture, or differentiation conditions, and provides an efficient platform to investigate biological mechanisms underlying specific phenomena and to perform pre-clinical screening studies of neurotrophic and neurotoxic agents.

References

1. Shipley MM, Mangold CA, Szpara ML. Differentiation of the SH-SY5Y Human Neuroblastoma Cell Line. *Journal of Visualized Experiments*. 2016;(108). doi:10.3791/53193
2. Zhao B, Schwartz JP. Involvement of cytokines in normal CNS development and neurological diseases: Recent progress and perspectives. *J Neurosci Res*. 1998;52(1):7-16. doi:10.1002/(SICI)1097-4547(19980401)52:1<7::AID-JNR2>3.0.CO;2-1
3. Xiao N, Le QT. Neurotrophic Factors and Their Potential Applications in Tissue Regeneration. *Arch Immunol Ther Exp (Warsz)*. 2016;64(2):89-99. doi:10.1007/s00005-015-0376-4
4. Biedler JL, Helson L, Spengler BA. Morphology and Growth, Tumorigenicity, and Cytogenetics of Human Neuroblastoma Cells in Continuous Culture1. *Cancer Res*. 1973;33(11):2643-2652. <http://aacrjournals.org/cancerres/article-pdf/33/11/2643/2390476/cr0330112643.pdf>
5. Ross RA, Spengler BA, Biedler JL. Coordinate Morphological and Biochemical Interconversion of Human Neuroblastoma Cells. *JNCI: Journal of the National Cancer Institute*. 1983;71(4):741-747. doi:10.1093/jnci/71.4.741
6. Dwane S, Durack E, Kiely PA. Optimising parameters for the differentiation of SH-SY5Y cells to study cell adhesion and cell migration. *BMC Res Notes*. 2013;6(1):366. doi:10.1186/1756-0500-6-366
7. Kovalevich J, Langford D. Considerations for the use of SH-SY5Y neuroblastoma cells in neurobiology. *Methods in Molecular Biology*. 2013;1078:9-21. doi:10.1007/978-1-62703-640-5_2
8. Cheung YT, Lau WKW, Yu MS, et al. Effects of all-trans-retinoic acid on human SH-SY5Y neuroblastoma as *in vitro* model in neurotoxicity research. *Neurotoxicology*. 2009;30(1):127-135. doi:10.1016/j.neuro.2008.11.001
9. Pählman S, Ruusala AI, Abrahamsson L, Odelstad L, Nilsson K. Kinetics and concentration effects of TPA-induced differentiation of cultured human neuroblastoma cells. *Cell Differ*. 1983;12(3):165-170. doi:10.1016/0045-6039(83)90006-4
10. Kim B, Leventhal PS, Saltiel AR, Feldman EL. Insulin-like Growth Factor-I-mediated Neurite Outgrowth *in Vitro* Requires Mitogen-activated Protein Kinase Activation. *Journal of Biological Chemistry*. 1997;272(34):21268-21273. doi:10.1074/jbc.272.34.21268
11. Encinas M, Iglesias M, Liu Y, et al. Sequential treatment of SH-SY5Y cells with retinoic acid and brain-derived neurotrophic factor gives rise to fully differentiated, neurotrophic factor-dependent, human neuron-like cells. *J Neurochem*. 2000;75(3):991-1003. doi:10.1046/j.1471-4159.2000.0750991.x

12. Ferlemann FC, Menon V, Condurat AL, Rößler J, Pruszak J. Surface marker profiling of SH-SY5Y cells enables small molecule screens identifying BMP4 as a modulator of neuroblastoma differentiation. *Sci Rep.* 2017;7(1):13612. doi:10.1038/s41598-017-13497-8
13. Katsatos CD, Herman MM, Mörk SJ. Class III β -tubulin in human development and cancer. *Cell Motil Cytoskeleton.* 2003;55(2):77-96. doi:10.1002/cm.10116
14. Pähnman S, Ruusala AI, Abrahamsson L, Mattsson MEK, Esscher T. Retinoic acid-induced differentiation of cultured human neuroblastoma cells: a comparison with phorbol-ester-induced differentiation. *Cell Differ.* 1984;14(2):135-144. doi:10.1016/0045-6039(84)90038-1
15. Kawabata M. Signal transduction by bone morphogenetic proteins. *Cytokine Growth Factor Rev.* 1998;9(1):49-61. doi:10.1016/S1359-6101(97)00036-1
16. Wang RN, Green J, Wang Z, et al. Bone Morphogenetic Protein (BMP) signaling in development and human diseases. *Genes Dis.* 2014;1(1):87-105. doi:10.1016/j.gendis.2014.07.005
17. Chen D, Zhao M, Mundy GR. Bone Morphogenetic Proteins. *Growth Factors.* 2004;22(4):233-241. doi:10.1080/08977190412331279890
18. Gilliam DT, Menon V, Bretz NP, Pruszak J. The CD24 surface antigen in neural development and disease. *Neurobiol Dis.* 2017;99:133-144. doi:10.1016/j.neurobiol.2016.12.011
19. Bekinschtein P, von Bohlen und Halbach O. Editorial: Cellular and Molecular Mechanisms of Neurotrophin Function in the Nervous System. *Front Cell Neurosci.* 2020;14. doi:10.3389/fncel.2020.00101
20. Chen BY, Wang X, Wang ZY, Wang YZ, Chen LW, Luo ZJ. Brain-derived neurotrophic factor stimulates proliferation and differentiation of neural stem cells, possibly by triggering the Wnt/ β -catenin signaling pathway. *J Neurosci Res.* 2013;91(1):30-41. doi:10.1002/jnr.23138
21. 2Brafman DA. Generation, Expansion, and Differentiation of Human Pluripotent Stem Cell (hPSC) Derived Neural Progenitor Cells (NPCs). In: *Stem Cell Renewal and Cell-Cell Communication.* Vol 1212. Springer New York; 2014:87-102. doi:10.1007/7651_2014_90
22. Jacob F, Pather SR, Huang WK, et al. Human Pluripotent Stem Cell-Derived Neural Cells and Brain Organoids Reveal SARS-CoV-2 Neurotropism Predominates in Choroid Plexus Epithelium. *Cell Stem Cell.* 2020;27(6):937-950. doi:10.1016/j.stem.2020.09.016
23. Agholme L, Lindström T, Kågedal K, Marcusson J, Hallbeck M. An *In Vitro* Model for Neuroscience: Differentiation of SH-SY5Y Cells into Cells with Morphological and Biochemical Characteristics of Mature Neurons. *Journal of Alzheimer's Disease.* 2010;20(4):1069-1082. doi:10.3233/JAD-2010-091363
24. Teppola H, Sarkanen JR, Jalonens TO, Linne ML. Morphological Differentiation Towards Neuronal Phenotype of SH-SY5Y Neuroblastoma Cells by Estradiol, Retinoic Acid and Cholesterol. *Neurochem Res.* 2016;41(4):731-747. doi:10.1007/s11064-015-1743-6

Keywords or phrases:

Artificial intelligence (AI), Label-free analysis, cytotoxicity assay, live-cell analysis, cell viability, advanced image analysis, chemotherapeutics, neuroscience

Quantifying Chemotherapeutic Cytotoxicity in Glial Cells using AI-Driven Label-Free Cell Analysis

Jasmine Trigg¹, Daniel Porto², Nevine Holtz², Nicola Bevan¹, Timothy Jackson¹, Timothy Dale¹, Gillian Lovell¹

1. Sartorius UK Ltd, Royston, Hertfordshire, UK

2. Sartorius Ann Arbor MI, USA

Correspondence

Email: AskAScientist@sartorius.com

Introduction

Glioblastoma multiform (GBM) is an aggressive glioma that originates from astrocytes and is associated with poor prognosis.¹ Several barriers exist in the treatment of GBM, including the localization of the tumor within the brain, a high rate of malignant invasion, tumor heterogeneity, and an intrinsic resistance to conventional therapies. Despite concerted efforts to overcome these, a lack of translational *in vitro* models and robust analytical tools makes deciphering the complex molecular interactions challenging.^{2,3}

Technological progression has facilitated the adoption of advanced cellular models, such as primary cells or induced pluripotent stem cells (iPSCs), that more precisely represent human phenotypes. This has simultaneously driven the requirement for label-free, non-perturbing analytical methods to accurately capture biologically relevant data in complex models and provide critical insights into disease processes.^{4,5} By eliminating fluorescent labels, this ensures that experimental observations are not attributed to the label, or the labeling process, and provides a method that is amenable to cell types where labeling is not feasible, such as sensitive or rare cells.^{6,7}

Find out more: www.sartorius.com/incipcyte-ai-cell-health-software

Live-cell imaging enables the acquisition of phase contrast images in a non-perturbing manner. Alongside the incorporation of Artificial Intelligence (AI) into image analysis workflows, this has empowered accurate quantification of a broad spectrum of cellular models, making it a powerful approach to make data-driven decisions and further understanding of cancer biology. These innovative technologies, based on neural network algorithms, are more complex than traditional image analysis and facilitate more accurate

segmentation of heterogenous cell morphologies whilst minimizing user-introduced bias.^{4,8}

In this application note, we describe a robust solution for label-free cell segmentation and live/dead classification of individual cells using integrated AI-based software. We exemplify how this approach can provide high-throughput insights into glial cell health in response to clinically relevant chemotherapeutic treatments.

Assay Principle

The Incucyte® AI Cell Health Analysis Software Module enables label-free quantification of cell viability. The analysis module uses trained convolutional neural networks (CNNs), which automatically analyzes phase contrast images to segment individual cells and classify them as live or dead, all in one step. This streamlined workflow (Figure 1) requires minimal user input, providing unbiased results which can be directly compared across assays.

Phase contrast images are acquired using AI Scan acquisition with 10X or 20X objectives in microplates up to

384-well throughput. These images can be analyzed using the Incucyte® AI Cell Health Analysis Software Module which provides metrics such as Total Cell Count (all objects), as well as the number and percentage of live and dead cells. In cases where optional fluorescence images are acquired, the mean and total integrated intensity within all cells, as well as within the live or dead subpopulations, will be provided. Fluorescence classification can be performed as an additional analysis, again providing metrics describing the count and percentage of high vs. low fluorescence within total cells, and within live or dead subpopulations.

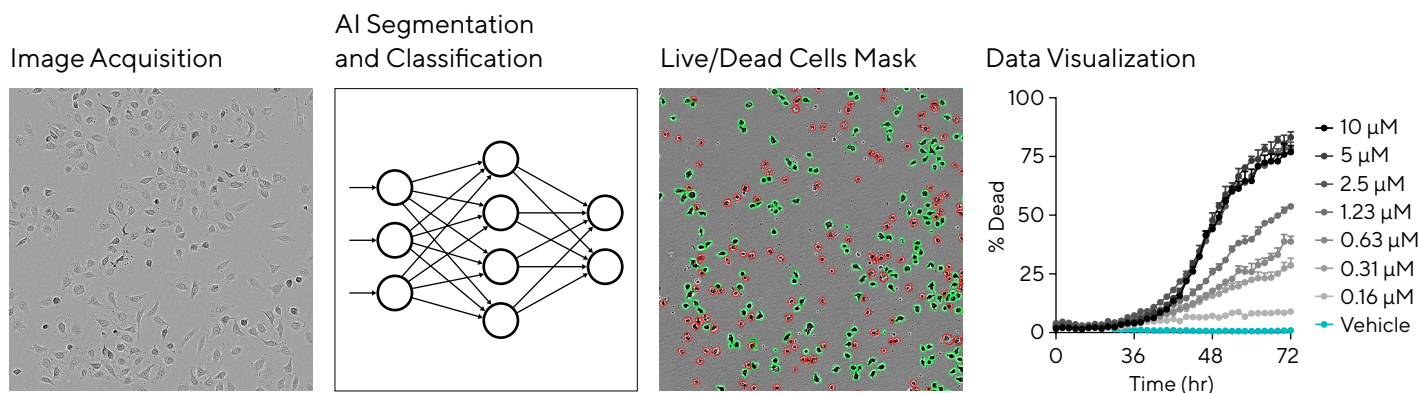


Figure 1: Incucyte® AI Cell Health Analysis Workflow.

Phase contrast images are acquired and processed using neural networks (CNN), to automatically segment and classify cells as live or dead.

Precise segmentation provides accurate cell count data even at high cell confluence and yields reliable proliferation data. Label-free classification of cells as live or dead enables quantification of cell viability within a physiologically relevant and non-perturbing environment. The combination of

label-free analysis with optional fluorescence readouts from the live or dead subpopulations provides additional insight into mechanisms of cell death.

AI-Driven Cell Segmentation

The AI Cell Health segmentation model was trained using phase contrast images which were manually annotated to identify the boundary of individual cells as described previously.^{9,10} The resulting segmentation is highly accurate and adaptable to numerous cell morphologies. Figure 2 shows the AI segmentation applied to different glial cell

types including an adherent glioblastoma cell line (A172), a semi-adherent microglial cell line (BV2), flat and transparent primary rat cortical astrocytes (Incucyte® rAstrocytes), and dead cells are accurately outlined (T98G cells treated with Taxol (paclitaxel, 500 nM)).

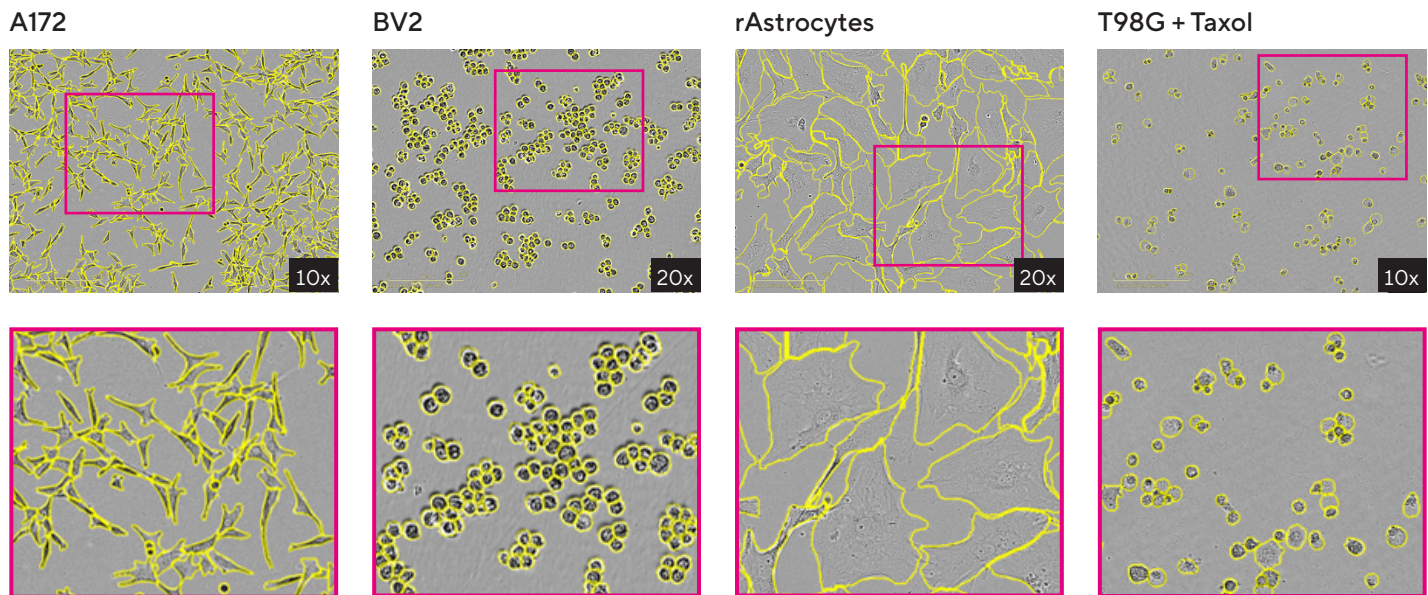


Figure 2: Incucyte® AI Cell Health Analysis Accurately Segments a Wide Range of Live and Dead Cell Types With Diverse Morphologies.

HD phase contrast images were acquired using the Incucyte® Live-Cell Analysis System at 10X or 20X magnification. AI Cell segmentation (yellow outline) shown for glial cell types.

AI-Driven Live/Dead Classification

AI Cell Health Analysis can identify live and dead cells without the requirement for a fluorescent reagent. For the validation of AI-driven classification, a wide range of cell types were treated with cytotoxic compounds in the presence of Incucyte® Cytotox Dye which enters non-viable cells, increasing their fluorescence intensity.¹⁰ Here, we demonstrate this validation process applied to glial cell lines of interest (Figure 3).

T98G glioblastoma cells, A172 glioblastoma cells, and BV2 microglia cells were treated with concentration ranges of compounds to induce cell death in the presence of Incucyte® Cytotox Green Dye (Figure 3). Quantification of cell death was performed using both Incucyte® AI Cell Health Live/Dead classification (AI-driven, label-free analy-

sis) and fluorescence classification of Cytotox positive cells. Phase and fluorescence blended images show live and dead cells for each cell type (Figure 3A). Time courses show percentage of dead cells in response to compound treatment and display comparable time- and concentration-dependent responses between fluorescence (Cytotox) and Incucyte® AI Cell Health classification (label-free) across all conditions tested (Figure 3B). Concentration response curves for T98G and A172 (72h) or BV2 cells (24h) confirm analogous compound efficacies using label-free and fluorescence analysis (Figure 3C). This confirms that the label-free Incucyte® AI Cell Health Analysis accurately identifies cell death induced by compounds with different mechanisms of action across a heterogenous group of glial cell types.

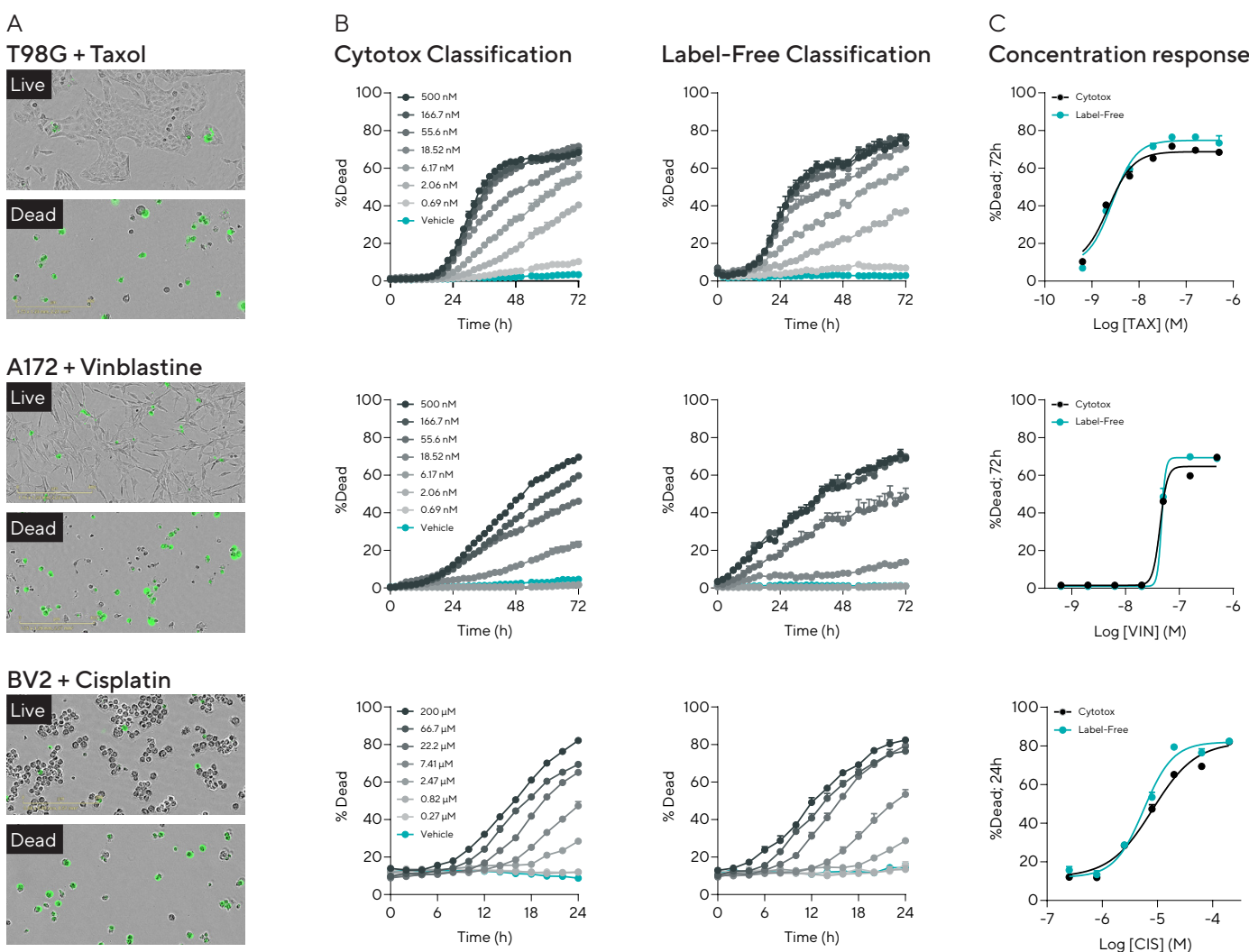


Figure 3: Incucyte® AI Cell Health Analysis Produces Cytotoxicity Data Comparable to Standard Fluorescence Methods.

A172, T98G, or BV2 cells were treated with concentration ranges of 3 different cytotoxic compounds in the presence of Incucyte® Cytotox Dye. Phase and fluorescence images are shown for live and dead cells for each cell type (A). Time courses show the percentage of dead cells over time using fluorescence classification (cytotox) or Incucyte® AI Cell Health Analysis (label-free). Concentration response curves plot cell death at 72 (T98G and A172) or 24 hours (BV2) (C). Data shown as mean \pm SEM, n= 3 replicates.

Chemotherapeutic Response of Glioblastoma Cells in Microplate Throughput

Genetic heterogeneity of GBM is well recognized and is considered a contributing factor in the lack of effective chemotherapy for new and recurrent disease.¹¹ The Akt-PI3K signaling pathway, which controls cell growth and survival, is negatively regulated by the tumor suppressor phosphatase and tensin homolog (PTEN).¹² Loss of PTEN function has been associated with uncontrolled proliferation and tumor resistance and PTEN is commonly deleted or mutated in up to 80% of GBMs.³ Information on genetic alterations and the mechanisms associated with tumor resistance has the potential to provide the fundamental basis for more precise or novel therapeutic strategies.

To examine drug sensitivity, we compared 3 glioblastoma cell lines with different PTEN expression status in their response to chemotherapeutic compounds with varied mechanisms of action. Initially, A172 (PTEN-negative³), T98G (PTEN expressing¹³), and U87-MG cells (PTEN-deficient¹⁴) were treated with 13 clinically relevant chemotherapeutics consisting of high and low concentrations in a 96-well plate (Figure 4). Microplate views of percentage of dead cells over time (Figure 4A) and heat maps at 72 hours (Figure 4B) were utilized to identify compound hits that suggested differential sensitivity across the three cell lines. Phase contrast images were used to confirm the detected levels of cell death (Figure 4C). For most compounds we observed that U87-MG had lower percentages of cell death compared to A172 and T98G cells, suggesting reduced compound sensitivity.

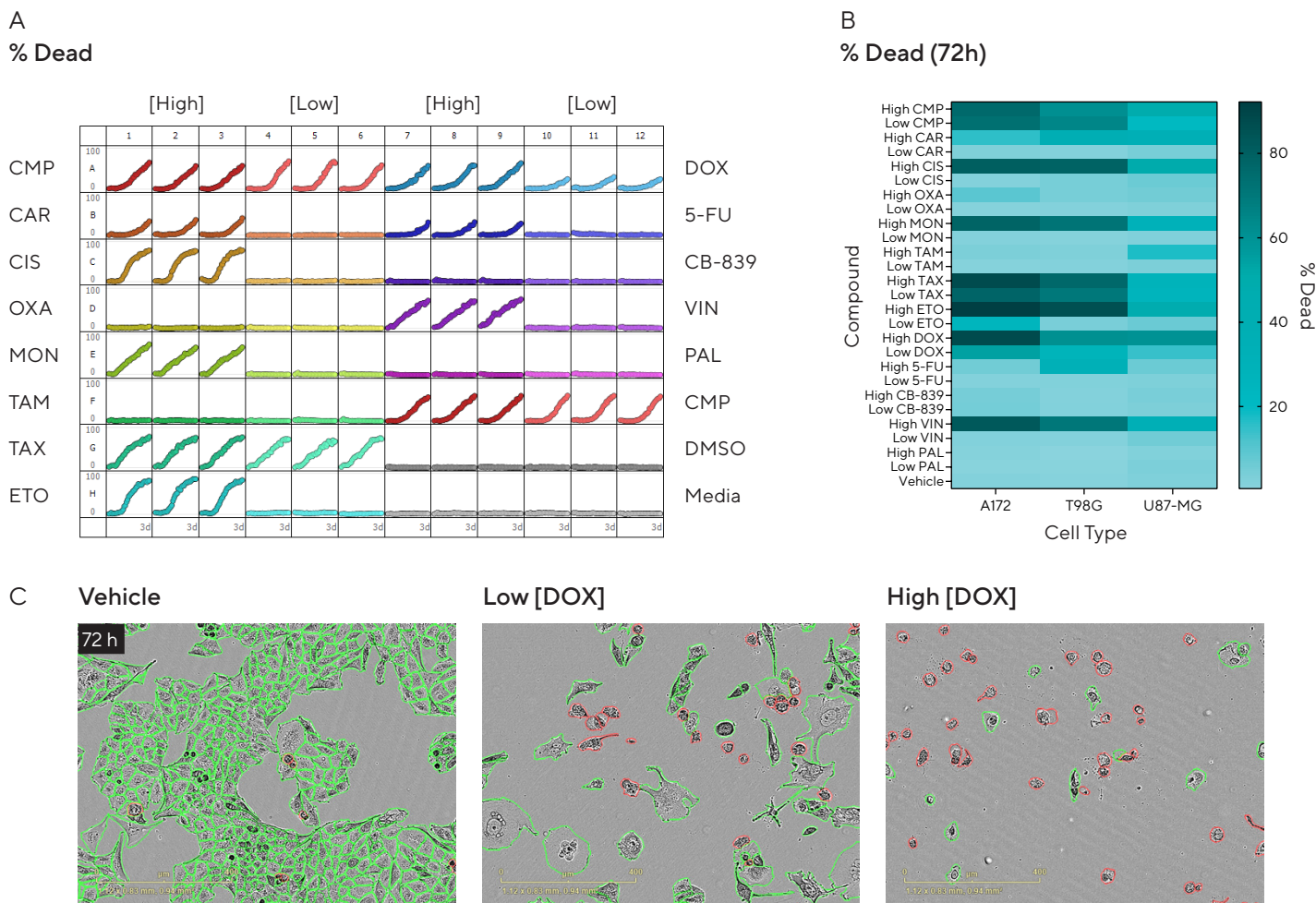


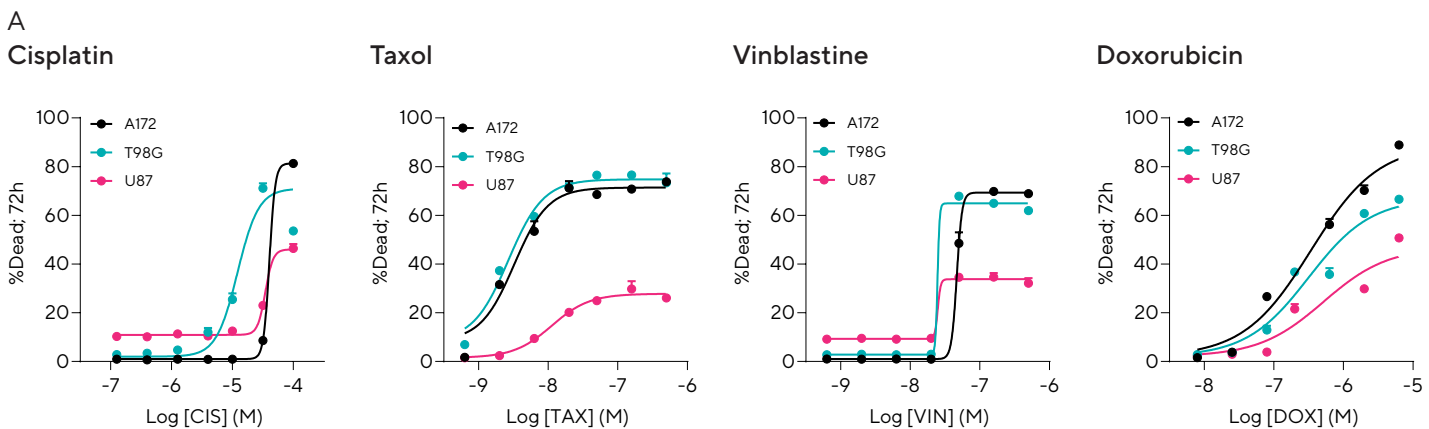
Figure 4: Label-Free Screening of Glioblastoma Responses to Chemotherapeutic Compounds in Microplate Format.

A172 (PTEN-negative), T98G (PTEN-expressing), and U87-MG (PTEN-deficient) glioblastoma cell lines were seeded into 96-well plates (2,000 cells/well) and once adhered, treated with high or low concentrations of 13 chemotherapeutic compounds. Microplate view shows the percentage of dead cells for T98G cells over 3 days (A). Heat map of the percentage of dead cells at 72 hours allows for comparison of compound toxicity across glioblastoma cell lines (B). Representative phase images show Incucyte® AI Cell Health Live (green) and Dead (red) classification masks for Doxorubicin (DOX) treated or vehicle T98G cells at 72 hours. Data shown as mean \pm SEM, n=3 replicates.

Four compounds were selected to investigate further based on observed differences in cell death. The glioblastoma cell lines were seeded into 96-well plates, treated with a 3-fold serial dilution of cisplatin, Taxol (paclitaxel), vinblastine, and doxorubicin, and cell death was monitored over 3 days (Figure 5). Concentration response curves (Figure 5A) for each compound are shown at 72 hours, with reported EC₅₀ and maximal percentage cell death values (Figure 5B). Data revealed differences in compound cytotoxic effects across cell lines and across compounds with different mechanisms of action, with U87-MG exhibiting reduced sensitivity compared to T98G and A172 cells for all compounds. For example, Taxol, a highly potent anti-cancer agent commonly used against solid tumors, induced comparable levels of

efficacy in A172 and T98G cells with maximal cell death values of 73.8 % and 76.6 %, respectively, and identical EC₅₀ values of 0.003 μ M. However, efficacy was reduced in U87-MG cells inducing maximal cell death of 27.1 % and an EC₅₀ value of 0.014 μ M.

This suggests that the PTEN status could be one of multiple factors, as part of complex regulatory signaling pathways, that modify the efficacy of these of compounds. Overall, the data highlights how label-free analysis can robustly be used to examine multiple conditions in high-throughput, with the potential to gain deeper insights into the genetic influences on drug resistance in an unbiased manner.



B

Compound	Mechanism of Action	A172		T98G		U87-MG	
		EC ₅₀ (μ M)	Max (%)	EC ₅₀ (μ M)	Max (%)	EC ₅₀ (μ M)	Max (%)
Cisplatin	DNA alkylating agent	40.6	80.5	12.7	70.8	36.5	43.8
Taxol	Inhibitor of microtubule dissociation	0.003	73.8	0.003	76.6	0.014	27.1
Vinblastine	Disrupts microtubule assembly	0.054	69.8	0.028	67.8	0.026	31.4
Doxorubicin	DNA intercalator; topoisomerase II inhibitor	0.33	88.9	0.52	66.6	0.69	46.5

Figure 5: Profiling Cell Death Responses to Concentration Ranges of Chemotherapeutic Compounds in Glioblastoma Cell Lines.

A172 (PTEN-negative), T98G (PTEN-expressing), and U87-MG (PTEN-deficient) cells were seeded into 96-well plates (2,000 cells/well) and once adhered treated with concentration range of Cisplatin, Taxol, Vinblastine, and Doxorubicin. Transformed data at 72 hours compares compound efficacies (A). Table reports EC₅₀ and maximal the percentage of dead cells values observed at 72 hours across all conditions studied (B). Data shown as mean \pm SEM, n= 3 replicates.

Label-Free Analysis Enables Examination of Compound Mechanisms of Action in Primary Astrocytes

Traditionally the field of neuro-oncology has heavily relied on tumor cell lines such as neuroblastomas or glioblastomas. Whilst these approaches remain useful, they have limited translational value and are unable to fully recapitulate the complexity and heterogeneity observed in brain tumors.

Consequently, there is an increase in the use of more sensitive or rare cell types, such as iPSCs and primary cells. To support drug discovery and accelerate these advanced models, the continued development of non-perturbing *in vitro* assays and analytical approaches are essential.

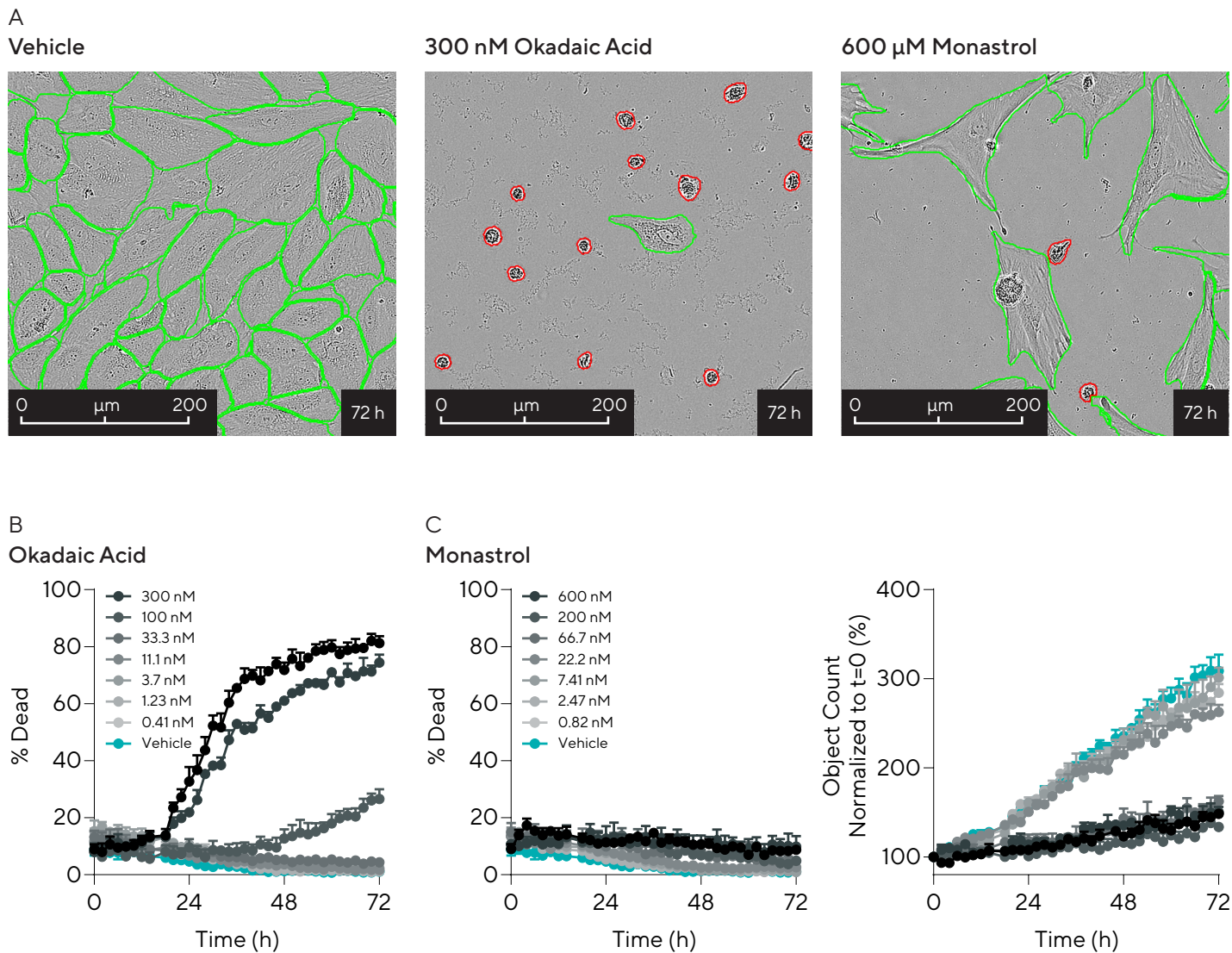


Figure 6: Label-Free Analysis of Compound Mechanisms of Action.

Primary rat cortical astrocytes (Incucyte® rAstrocytes) were seeded onto Poly-L-Lysine (PLL) coated 96-well TPP plates (2,500 cells/well) and treated with a concentration range of okadaic acid or Monastrol. Cell death was quantified using Incucyte® AI Cell Health Analysis Software Module. Images of vehicle and drug-treated conditions show AI Live (green) and Dead (red) classification masks and enable visualization of morphological changes (A). Time course shown for okadaic acid quantifying the percentage of dead cells (B). Time courses shown for % dead and total cell count for Monastrol (C). Data shown as mean \pm SEM, n= 3 replicates.

To demonstrate the utility of this label-free analysis we investigated mechanisms of drug action in primary astrocytes. Rat cortical astrocytes were treated with a concentration range of two compounds, okadaic acid (dual protein phosphatase inhibitor) and Monastrol (small molecule inhibitor of kinesin-5) and were monitored over 3 days using the Incucyte® Live-Cell Analysis System (Figure 6). Images at 72 hours post-treatment show AI Live and Dead classification and revealed okadaic acid (300 nM) induced cell death whilst Monastrol (600 μ M) was not toxic but induced morphological changes compared to vehicle (Figure 6A).

Quantification of cell death showed okadaic acid had a concentration-dependent cytotoxic effect on the primary astrocytes (Figure 6B). In contrast, Monastrol exerted an all-or-nothing cytostatic effect as revealed by little-to-no cell death but a reduction in cell proliferation (object count) with increasing compound concentrations (Figure 6C). This is consistent with known mechanisms of action and exemplifies how this assay is amenable to examination of compound effects in non-perturbing physiologically relevant conditions.

Combined Live-Cell Analysis and Flow Cytometry Approach Yields Additional Insights into Cell Death

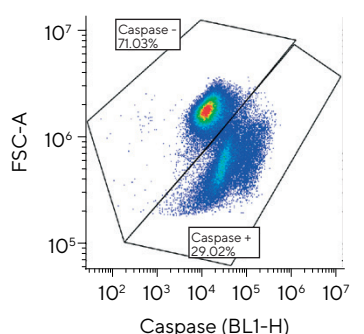
In the central nervous system, microglia primarily function as phagocytes in responding to infection or damage. Under pathological conditions, glioma associated microglia play an important role in the tumor microenvironment by responding to oncogenic signaling via the secretion of chemokines and cytokines that further promote tumor progression.¹⁵ Research is focusing on expanding our understanding of these biological roles and interactions, with therapies targeting microglia showing potential complements to current treatments.¹⁶

We used a combined approach of live-cell analysis and advanced flow cytometry to examine cell death in a microglial cell line. Incucyte® AI Cell Health Analysis Software Module enables label-free real-time monitoring of cell death and is non-exhaustive, which facilitates end-point selection and allows for downstream experiments to be performed to probe deeper into mechanisms of cell death. The iQue® Human 4-Plex Apoptosis Kit is a flow-cytometry based multi-parameter assay that enables quantification of four different apoptosis measurements per well including caspase 3/7 activity, annexin V binding, cell viability, and mitochondrial membrane potential (MMP) (Figure 7).

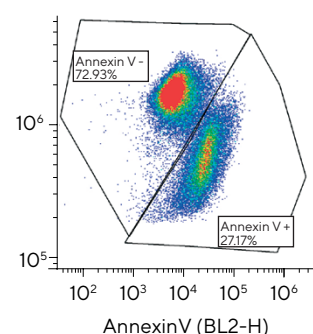
BV2 cells were treated with 3 chemotherapeutics, camptothecin (CMP), cisplatin (CIS), and carboplatin (CAR), all of which are known to cause DNA damage and activate apoptotic pathways.^{17,18} Images were acquired every 2 hours and cell death monitored using the Incucyte® Live-Cell Analysis System. At 24 hours post-treatment, cells were harvested and labeled with the iQue® Apoptosis Kit using a no-wash protocol. The samples were assessed on the iQue® Advanced Flow Cytometry Platform and analyzed using integrated Forecyt® Software. The data in Figure 7 highlights the gating strategy used for each of the apoptosis readouts (Figure 7A). The Forecyt® heat map shows concentration dependent increases in the percentage of caspase positive cells in response to camptothecin and cisplatin, with a partial increase observed for carboplatin (Figure 7B). We observed similar responses across all four apoptosis readouts (data not shown). Comparison of the concentration response curves between Incucyte® label-free and iQue® caspase positive readouts revealed analogous results in compound efficacy (Figure 7C). Taking camptothecin as an example, we observed EC₅₀ values of 0.35 and 0.34 μ M, respectively. This approach could also be used to examine each apoptosis pathway in more detail for example through assessing caspase-dependent or independent mechanisms.

A

Caspase3/7

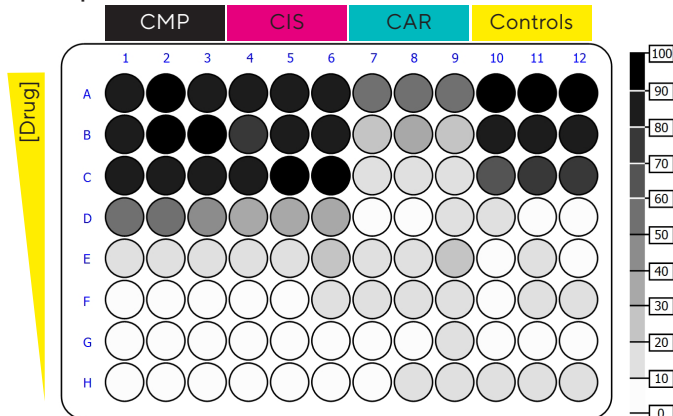


Annexin V

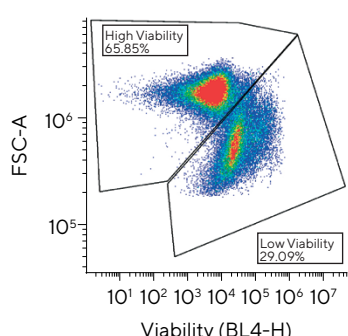


B

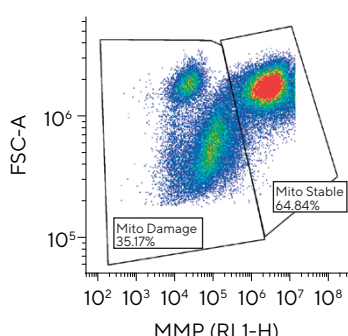
% Caspase +



Viability

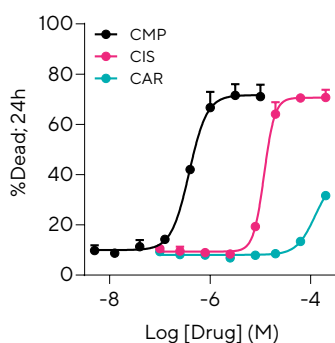


MMP



C

Incucyte® AI Cell Health



iQue® Caspase

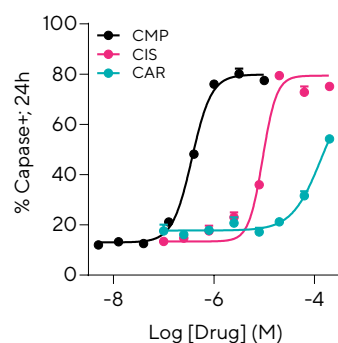


Figure 7: Combined Approach to Quantify Cell Death in Microglia Using Live-Cell Analysis and Flow Cytometry.

BV2 microglia cells were seeded onto a poly-L-ornithine (PLO) coated 96-well plate (8,000 cells/well) and once adhered treated with concentration ranges of camptothecin (CMP), cisplatin (CIS) and carboplatin (CAR). Images were acquired every 2 hours in the Incucyte® Live-Cell Analysis System over 24 hours and cell death quantified using Incucyte® AI Cell Health Analysis Software Module. At 24 hours, cells were harvested, transferred to a 96-well v-bottomed plate, labeled using the iQue® 4-Plex Apoptosis Kit (Cat. No. 90053) and run on the iQue® Advanced Flow Cytometry Platform. Dot plots show gating strategy used for each apoptosis readout (A). Heat map of 96-well plate shows caspase positive cells expressed as a percentage of single cells (B). Transformed data shows EC₅₀ curves for Incucyte® quantifying the percentage of dead cells and iQue® showing the percentage of caspase positive cells at 24 hours (C). Data shown as mean ± SEM, n = 3 replicates.

Summary & Conclusion

The response of tumor cells, such as glioblastomas, to cytotoxic chemotherapeutic compounds is a complex and dynamic process that is crucial to understand in neuro-oncology research. The Incucyte® AI Cell Health Analysis Software Module uses pre-trained neural networks to accurately segment individual cells and classify them as live or dead. The data shown demonstrates that this is a

powerful, robust approach for assessing cytotoxicity in glial cell types and is amenable to screening of therapeutic candidates. The label-free analysis enables non-perturbing quantification of cytotoxicity, which is especially important when using sensitive cell types, and enables downstream experiments, such as flow cytometry, to be performed for additional insights into the mechanisms of apoptosis.

References

1. Robins, H. I., Chang, S., Butowski, N., and Mehta, M. Therapeutic advances for glioblastoma multiforme: current status and future prospects. *Curr Oncol Rep*, 9, 66-70 (2007).
2. Thomas, A. A., Brennan, C. W., DeAngelis, L. M., and Omuro, A., M. Emerging Therapies for Glioblastoma. *JAMA Neurol* (2014).
3. Zhang, A., Banik, L., and Ray, S. Differential sensitivity of human glioblastoma LN18 (PTEN-positive) and A172 (PTEN-negative) cells to Taxol for apoptosis. *Brain research*, 1239, 216-255 (2008).
4. Hillger, J.M., Lieuw, W.L., Heitman, L.H. and IJzerman, A.P. Label-free technology and patient cells: from early drug development to precision medicine. *Drug Discovery Today*, 22(12), 1808-1815 (2017).
5. Kusumoto, D., Yuasa, S., Fukuda, K. Induced Pluripotent Stem Cell-Based Drug Screening by Use of Artificial Intelligence. *Pharmaceuticals*, 15, 562 (2022).
6. Baens, M. et al. The dark side of EGFP: defective polyubiquitination. *PLoS ONE* 1, e54 (2006).
7. Cekanova, M. & Rathore, K. Animal models and therapeutic molecular targets of cancer: utility and limitations. *Drug Des. Devel. Ther.* 8, 1911-1922 (2014).
8. Ayers MA, Jayatunga M, Goldader J, Meier C. Adopting AI in Drug Discovery. Boston Consulting Group. Retrieved January 05, 2022. <https://www.bcg.com/publications/2022/adopting-ai-in-pharmaceutical-discovery>
9. Edlund, C., Jackson, T.R., Khalid, N., Bevan, N., Dale, T., Dengel, A., Ahmed, S., Trygg, J., Sjögren, R. LIVECell: A large-scale dataset for label-free live cell segmentation. *Nat. Methods*, 18, 1038-1045 (2021).
10. Trigg, J., Porto, D., Holtz, N., Bevan, N., Jackson, T., Dale, T., and Lovell, G. AI-Driven Label-Free Quantification of Cell Viability Using Live-Cell Analysis (2023).
11. Montaldi, A., Lima, S., Godoy, P., Xavier, D., and Sakamoto-Hojo, E. PARP-1 inhibition sensitizes temozolamide-treated glioblastoma cell lines and decreases drug resistance independent of MGMT activity and PTEN proficiency. *Oncology Reports*, 44, 2275-2287 (2020).
12. Benitez, J. A. et al. PTEN regulates glioblastoma oncogenesis through chromatin-associated complexes of DAXX and histone H3.3. *Nature Communications*, 8 (2017).
13. Milella, M. et al. PTEN status is a crucial determinant of the functional outcome of combined MEK and mTOR inhibition in cancer. *Scientific Reports*, 7 (2017)
14. Lee, J. J. et al. PTEN status switches cell fate between premature senescence and apoptosis in glioma exposed to ionizing radiation. *Cell Death and Differentiation*, 18, 666-677 (2011).
15. Hambardzumyan, D., Gutmann, D. H., Kettenmann, H. The role of microglia and macrophages in glioma maintenance and progression. *Nat Neurosci*, 19, 20-7 (2015). doi: 10.1038/nn.4185
16. Geribaldi-Dolan, N. et al. The role of Microglia in Glioblastoma. *Frontiers in Oncology* (2021). Doi: 10.3389/fonc.2020.603495
17. Morris, E. J., and Geller, H. M. Induction of neuronal apoptosis by camptothecin, an inhibitor of DNA topoisomerase-I: evidence for cell cycle-independent toxicity. *J Cell Biol*, 134, 757-70 (1996).
18. Unger, F., Klasen, H., Tchartchian, G., de Wilde, R., and Witte, I. DNA damage induced by cis- and carboplatin as indicator for *in vitro* sensitivity of ovarian carcinoma cells. *BMC Cancer*, (2009). doi:10.1186/1471-2407-9-359

North America

Sartorius Corporation
300 West Morgan Road
Ann Arbor, Michigan 48108
USA
Phone +1734 769 1600
Email: orders.US07@sartorius.com

Europe

Sartorius UK Ltd.
Longmead Business Centre
Blenheim Road
Epsom
Surrey, KT19 9QQ
United Kingdom
Phone +44 1763 227400
Email: euorders.UK03@sartorius.com

Asia Pacific

Sartorius Japan K.K.
4th Floor, Daiwa Shinagawa North Bldg.
1-8-11, Kita-Shinagawa 1-chome
Shinagawa-Ku
Tokyo 140-0001
Japan
Phone +81 3 6478 5202
Email: orders.US07@sartorius.com

 **Find out more:** www.sartorius.com/incucyte

 **For questions, email:** AskAScientist@sartorius.com

Keywords or phrases:

ALS, Neurodegenerative, iPSC, Immunocytochemistry, Neuronal Activity, Phagocytosis, Motor Neurons, Microglia, Live-Cell Analysis

iPSC-Derived Motor Neurons and Microglia From ALS Background Display Disease Phenotype

Jessica Tilman

Axol Bioscience Ltd, Roslin Innovation Centre, Charnock Bradley Building, Easter Bush Campus, Easter Bush EH25 9RG UK

Correspondence

Email: AskAScientist@sartorius.com

Abstract

Amyotrophic lateral sclerosis (ALS) is a neurodegenerative disorder caused by the degeneration of motor neurons, and ultimately results in death. Despite the fatal nature of this disease, there is no current cure or effective treatment available. The clear overlap between ALS and Frontotemporal Dementia (FTD) has led to the belief that it is not only disruption in motor neurons which drives ALS symptoms, but other cell types such as microglia, the main immune cell found in the brain, may also play a role. To investigate this, fibroblasts taken from a healthy individual and an ALS patient carrying a C9orf72 hexanucleotide expansion (GGGGCC >145) were reprogrammed to Induced Pluripotent Stem Cells (iPSCs), and then differentiated to motor neurons and microglia alongside controls. The cells were then assessed for differences in morphology and functional activity, measured via electrophysiology, spontaneous neural activity, and microglial phagocytosis. Diseased iPSC-derived motor neurons exhibited less organized morphology compared to control, as well as less synchronized firing patterns and hyperexcitability. ALS patient-derived microglia demonstrated a decreased capability for phagocytosis, particularly when cryopreserved. Taken together, these results demonstrate clear morphological and functional differences in differentiated cells derived from a C9orf72-positive ALS patient, compared to healthy control cells which can therefore be used as a robust model for C9orf72 ALS research and drug discovery.

 For further information, visit www.sartorius.com

Introduction

Amyotrophic lateral sclerosis (ALS) is a neurodegenerative disorder caused by the degeneration of motor neurons, and ultimately results in death on average 2-3 years after onset of symptoms. 5-10% of ALS cases have a familial background with an autosomal dominant inheritance pattern. Of these, mutations in C9orf72 account for the highest number of cases¹. Sporadic ALS accounts for the remaining cases, with a high degree of them containing identifiable genetic causes. There is a clear overlap between ALS and FTD with approximately 5% of ALS patients showing overt characteristics of FTD, and up to 50% showing more subtle similarities². This observation has led to the belief that it is not only disruption in motor neurons which drives ALS symptoms, but other cell types play an important role too. Microglia are the main immune cell found in the brain, with key roles in maintaining neuronal homeostasis as well as driving inflammatory responses³. Changes in inflammatory response and phagocytosis have been heavily implicated in neurodegeneration and FTD, and more recently have been shown to be defective in ALS. C9orf72 mutation has been shown to drive an exaggerated immune response in microglia and lead to impaired phagocytosis and excitotoxicity in motor neurons^{3,4}.

ALS has an incidence rate of 2:100,000 per year, and despite the fatal nature of this disease, there is no current cure or effective treatment available¹. There has been significant progress in the field with greater understanding of the genetics, pathology, and biomarkers of ALS, but development of novel and effective therapies has in part been hindered by a lack of relevant and translational pre-clinical models. Understanding how different cell types become impaired and drive the development and progression of ALS is crucial in developing novel and effective treatments.

Use of relevant pre-clinical models is essential in not only understanding disease onset and progression, but also in gaining insight into the functionality of potential new treatments. ALS is a heterogeneous condition, and as such one treatment plan is unlikely to work for all patients. Mouse models are limited in this respect, as in most cases they rely on genetic modification or silencing of a key gene and would therefore only apply to patients with the same mutation. iPSC-derived models provide a relevant human platform which is reproducible and scalable. More importantly, the ability to reprogram samples directly from affected individuals allows for patient stratification based on not only genetic factors, but also on defined symptoms. This is invaluable in determining which treatments may work more effectively for subpopulations of patients with ALS and drive more effective clinical trials.

An additional benefit of using iPSC-derived cells is the ability to differentiate these cells towards different lineages

and generate several cell types which all contribute to development of ALS. Motor neurons harbouring a C9orf72 mutation are known to be hyperexcitable and to become dysfunctional in ALS. However, C9orf72 is most highly expressed in myeloid cells, implying an important contribution from these cells. Using iPSC-derived motor neurons and microglia from the same patient background enables for the study of these cells in isolation as well as in co-culture.

Method and Assays

axoLines™ iPSCs:

Fibroblasts taken from a healthy individual and an ALS patient carrying a C9orf72 hexanucleotide expansion (GGGGCC >145) were reprogrammed to iPSCs using Sendai virus or episomal vector.

axoCells™ iPSC-Derived Motor Neurons:

To generate mature motor neurons, iPSCs were differentiated to axoCells motor neuron progenitor cells (ax0078 and ax0074). Progenitor cells were generated in monolayer using small molecule induction methods. Progenitors were then matured to motor neurons for up to 20 days using the Axol Bioscience methodology to include neural media with the addition of Axol Bioscience motor neuron accelerator (ax0072 and ax0179). Motor neurons were characterized by immunocytochemistry, showing expression of HB9, LIM3, OLIG2, and TUJ1 by day 104 of maturation.

axoCells™ iPSC-Derived Microglia:

iPSCs were differentiated to macrophage-precursors by mesoderm induction via the formation of embryoid bodies. Precursor cells were characterised by flow cytometry for key macrophage/monocyte markers (CD14, CD11b, and CD16) before maturing the cells to microglia for a further 7 days using a cocktail of growth factors. At day 7 cells were either used for assays or cryopreserved. Upon thaw, cryopreserved microglia were plated on cell culture plates coated with Surebond XF and Concanavalin A and matured for a further 7 days before performing assays. Fresh and cryopreserved microglia were characterized by immunocytochemistry for expression of key microglia markers TMEM119, P2RY12, CX3CR1, and Iba1.

Immunocytochemistry:

Cells were fixed using 4% PFA for 10 minutes and washed in phosphate buffered saline (PBS). Cells were permeabilised using 1% Triton X and blocked in buffer containing Tween 20 and Donkey serum. Cells were then stained with primary antibodies for 2 hours at room temperature (RT) and washed twice using PBS-Tween. Secondary antibodies conjugated to FITC or AF-594 were then added for a further 2 hour incubation at RT. All wells were treated with ProLong™ Gold Antifade reagent containing DAPI and imaged using a Leica microscope.

Multi-Electrode Array (MEA):

Motor neuron progenitor cells were seeded at 150,000 cells/cm² in 48 well Axion CytoView MEA plates coated with vitronectin. Neurons were matured for 10 days, and MEA recordings of spontaneous firing taken throughout this process using an Axion Maestro Pro system. Recordings were analyzed to provide information on neuronal activity, burst firing, and synchronicity.

Spontaneous Neuronal Activity (SNA):

On day two of maturation of motor neurons, cells were transfected with Incucyte® Neuroburst Orange Lentivirus (Sartorius, Cat. no. 4736), a lentiviral based live-cell neuronal labeling reagent driven by a synapsin promoter, leading to the long term expression of an orange fluorescent calcium indicator. Motor neurons were imaged daily up to day 21 of maturation. Images were acquired using an Incucyte® S3 Live-Cell Analysis System configured with an Orange/NIR optical module and integrated Incucyte® Neuronal Activity Analysis Software Module was used to determine metrics of spontaneous neuronal activity.

Phagocytosis:

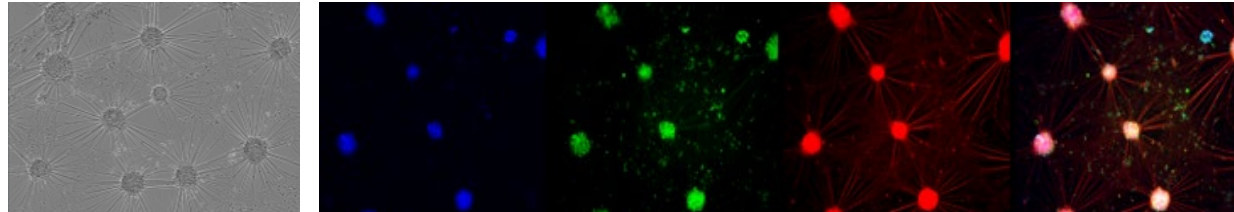
Myelin basic protein (MBP) was labeled with pHrodo® Orange Cell Labeling Dye for Incucyte® (Sartorius, Cat. no.: 4766) following the manufacturer's specifications. Labeled MBP was used as bait for microglia. Briefly, microglia were seeded in 384 well plates and matured for 7 days. On day 7, bait was added to each well and imaged using an Incucyte® S3 Live-Cell Analysis System for up to 24 hours. Cytochalasin D was added to control wells 30 minutes prior to addition of bait.

iPSC-Derived Motor Neuron Morphology

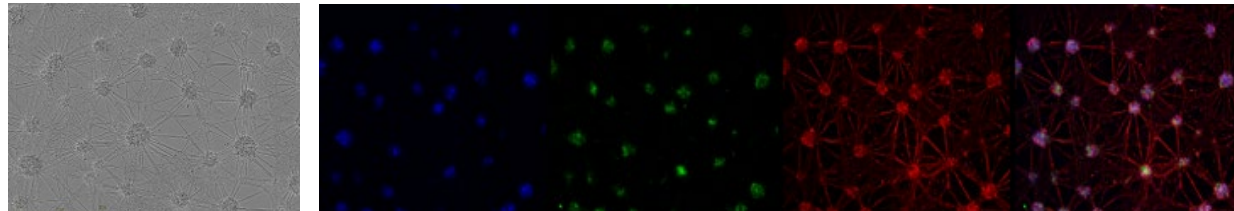
axoCells™ iPSC-derived motor neurons undergo quality control by staining for key markers such as CHAT, TUJ1, and HB9

(not shown) to ensure maturity (Figure 1). While these markers are present in both control and ALS motor neurons, the morphology of the neuronal networks shows differences between the two, indicating a disease driven phenotype. Control motor neurons form large clusters of cell bodies connected by strong cabling networks formed by neurites. In comparison, ALS motor neurons form many smaller clusters across the culture with a more disordered network formation. This could drive the hyperexcitability observed in ALS motor neuron cultures and explain in part the loss of synchronicity in this population.

Ax0078 (control)



Ax0074 (ALS C9orf72)



Phase contrast

Blue: DAPI

Green: HB9

Red: TUJ1

Merge

Figure 1: Mature axoCells™ iPSC-derived motor neurons (control and ALS) immunocytochemistry. Cells were matured for 20 days and stained for markers of motor neurons. DAPI was used as a nuclear dye.

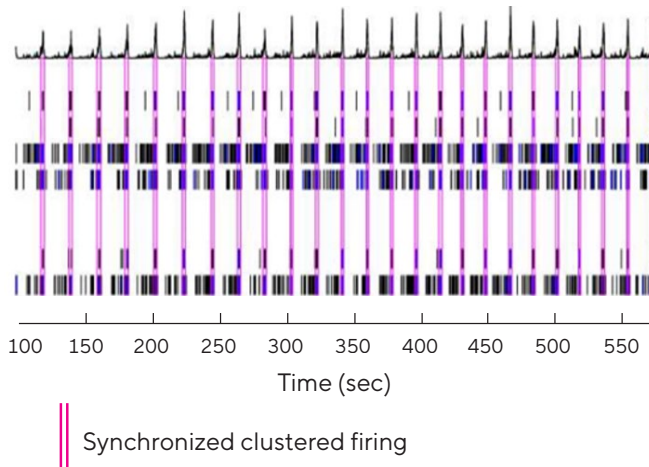
axoCells™ ALS Derived Motor Neurons Display Hyperexcitability Across Several Assay Platforms

There are several methods that can be used to assess neuronal function *in vitro*, one of which is using a multi electrode array (MEA) system. The functional behavior of neuronal networks can be captured to investigate electrical activity by measuring spontaneous action potentials (field potentials). Using this system, electrical activity can be compared between healthy and disease motor neurons to identify patterns of firing which contribute to the disease phenotype. In this way, a 'disease phenotype' can be defined and used to test potential drug candidates that may lead to a return to normal firing in motor neurons from a disease background.

axoCells™ Motor Neuron (control-derived)



Motor Neuron MEA Sodium Spike Profile



Motor neurons from control and ALS patient backgrounds were assessed using an Axion MEA system and demonstrated a clear disease phenotype (Figure 2). Control neurons exhibited regular and synchronized firing while ALS neurons showed more random clustered firing. This can be observed in the field potential traces (top) and in the raster plot (bottom). This disease phenotype is in line with the physiological dysfunction observed in neurons from ALS patients, including hyperexcitability and a loss of synchronicity within the cell population.

axoCells™ Motor Neuron (ALS-derived)



Motor Neuron MEA Sodium Spike Profile

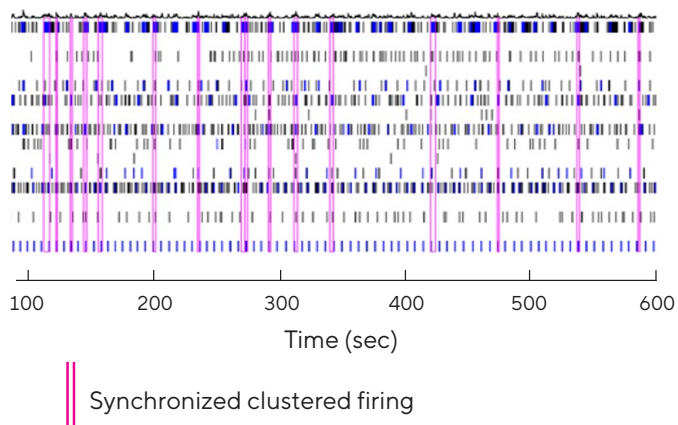
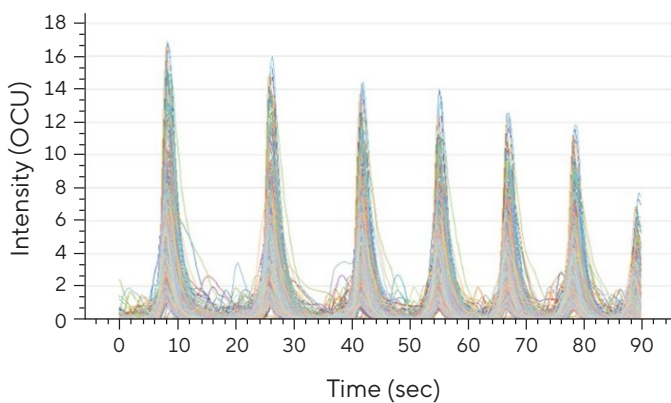


Figure 2: MEA recordings of day 10 mature motor neurons from healthy and ALS patients. Traces of activity detected for each cell line (top) and raster plot (bottom) demonstrating the difference in firing frequency and synchronicity.

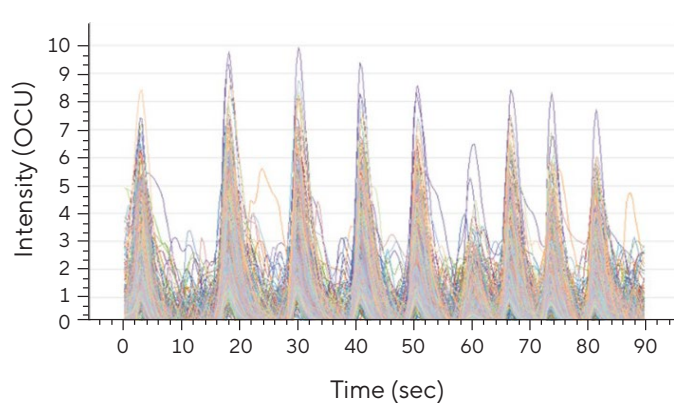
Another method to assess neuronal function is to interrogate the function of the whole well, as opposed to MEA in which a certain number of electrodes provide the information for the cell networks directly on them. Spontaneous neuronal activity can be measured using the Incucyte® Neuronal Activity Assay, wherein cells are monitored daily over the maturation process. Cells are transfected with Incucyte® Neuroburst Orange Lentivirus, a genetically-encoded calcium sensor, resulting in long term non-perturbing expression in neuronal cell types.

Using integrated software, calcium flux can then be kinetically measured as a readout for spontaneous neuronal activity and enabling assessment of burst rate, burst duration, and synchronicity (mean correlation) to investigate functional differences between cell lines. Data obtained from healthy- and ALS-derived motor neurons shows that control neurons have a regular and synchronized firing pattern while ALS neurons fire more frequently and with reduced synchronicity (Figure 3 A). ALS motor neurons exhibited significantly higher burst rate compared to the control line, along with lower burst duration and lower mean correlation (hence less synchronized burst firing) (Figure 3 B).

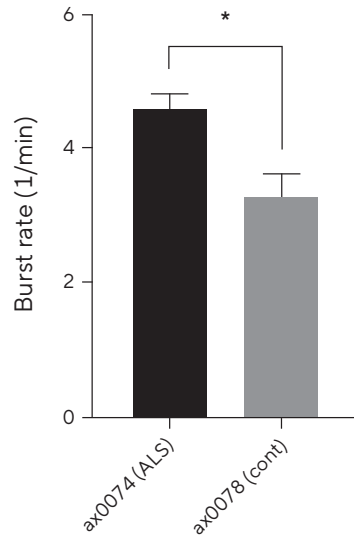
A) axoCells™ Motor Neuron



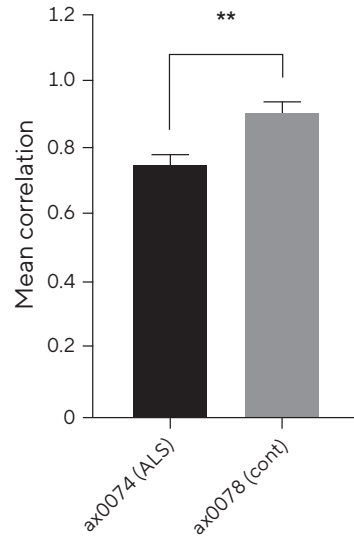
axoCells™ Motor Neuron



B) Mean Burst Rate



Mean Correlation



Mean Burst Duration

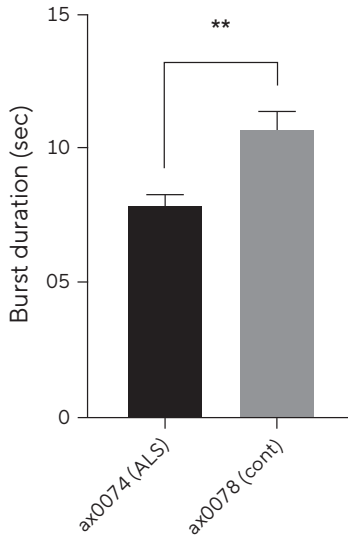


Figure 3: Spontaneous neuronal activity assay on day 18 motor neurons. Calcium signalling was monitored and analysed using the Incucyte® Neuronal Activity Software Module. A) Burst patterns for control and ALS motor neurons. B) Neuronal activity analysis for calcium signalling. Statistical significance was assessed using a non-parametric T-test, * $p<0.05$, ** $p<0.01$.

ALS Disease Phenotype is Observed in Microglia Phagocytosis

iPSC-derived microglia provide a platform to investigate how the immune response contributes to neurodegeneration and thus can be used for disease modeling and drug discovery. axoCells™ iPSC-derived microglia show expression of key markers by immunocytochemistry, including TMEM119, Iba1, P2RY12, and CX3CR1. Using iPSC-derived microglia, a clear difference could be observed in the capability of these cells to uptake myelin basic protein (MBP) with significantly higher phagocytosis in healthy cells compared to those from an ALS patient (Figure 4).

In addition, ALS microglia were more sensitive to the cryopreservation process, with the difference between healthy and disease cells exacerbated in thawed cells. Together this data indicate that ALS microglia are affected by the C9orf72 expansion in ALS with decreased phagocytosis and potentially becoming more sensitive to stresses such as cryopreservation.

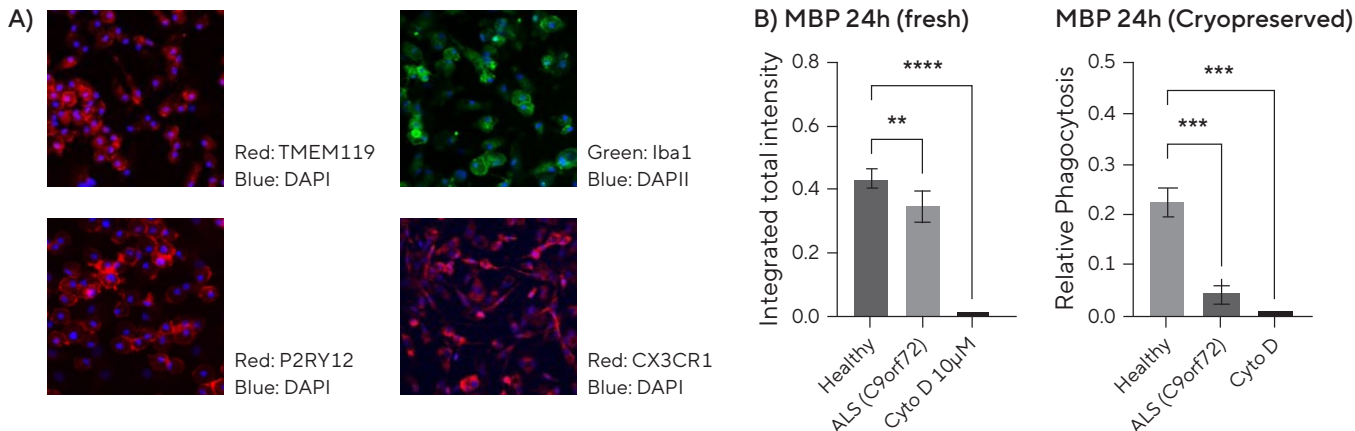


Figure 4: axoCells™ iPSC-derived microglia characterized by A) immunocytochemistry for key markers (representative images); B) phagocytosis of pHrodo® for Incucyte® labeled Myelin Basic Protein (MBP) was assessed on an Incucyte® Live-Cell Analysis System up to 24h using fresh and cryopreserved microglia. Cytochalasin D (10 µM) was used as a control. Statistical significance was assessed using a one-way ANOVA, **p<0.01, ***p<0.001, ****p<0.0001.

Summary & Outlook

iPSC-derived cells provide a valuable tool for disease modelling, with the ability to use cells directly from affected patients, as well as the potential to drive these cells towards multiple lineages. In this study, axoCells™ motor neurons and microglia from the same healthy and ALS axoLines™ iPSCs were shown to exhibit disease phenotypes which can be quantified and used for future drug discovery purposes. Further characterization of both cell types could elucidate additional functional dysregulation compared to healthy cells which may provide valuable insight into future potential treatments. In addition to understanding disease phenotype for each cell type, the potential to develop a co-culture system would add value in determining how these cells interact and whether both microglia and motor neurons from ALS patients could drive a more pronounced disease phenotype.

References

1. Mead, R.J., Shan, N., Reiser, H.J. et al. Amyotrophic lateral sclerosis: a neurodegenerative disorder poised for successful therapeutic translation. *Nat Rev Drug Discov* 22, 185–212 (2023). <https://doi.org/10.1038/s41573-022-00612-2>
2. Poulomi Banerjee et al. Cell-autonomous immune dysfunction driven by disrupted autophagy in C9orf72-ALS iPSC-derived microglia contributes to neurodegeneration. *Sci. Adv.* 9, eabq0651(2023). DOI: 10.1126/sciadv.abq0651
3. J. Brettschneider, J. B. Toledo, V. M. van Deerlin, L. Elman, L. McCluskey, V. M.-Y. Lee, J. Q. Trojanowski, Microglial activation correlates with disease progression and upper motor neuron clinical symptoms in amyotrophic lateral sclerosis. *PLOS ONE* 7, e39216 (2012).
4. O. Dols-Icardo, V. Montal, S. Sirisi, G. López-Pernas, L. Cervera-Carles, M. Querol-Vilaseca, L. Muñoz, O. Belbin, D. Alcolea, L. Molina-Porcel, J. Pegueroles, J. Turón-Sans, R. Blesa, A. Lleó, J. Fortea, R. Rojas-García, J. Clarimón, Motor cortex transcriptome reveals microglial key events in amyotrophic lateral sclerosis.

Note: axoCells™ and axoLines™ are registered trademarks of Axol Bioscience

North America

Sartorius Corporation
565 Johnson Avenue
Bohemia, NY 11716
USA
Phone +1 734 769 1600
Email: orders.US07@sartorius.com

Europe

Sartorius UK Ltd.
Longmead Business Centre
Blenheim Road
Epsom
Surrey, KT19 9QQ
United Kingdom
Phone +44 1763 227400
Email: eurordersUK03@sartorius.com

Asia Pacific

Sartorius Japan K.K
4th Floor, Daiwa Shinagawa North Bldg.
1-8-11, Kita-Shinagawa 1-chome
Shinagawa-Ku
Tokyo 140-0001
Japan
Phone +813 6478 5202
Email: eurordersUS07@sartorius.com

Axol Bioscience Ltd

Roslin Innovation Centre,
Charnock Bradley Building,
Easter Bush Campus, Easter
Bush EH25 9RG UK

For further information, visit
www.sartorius.com